DALTON
FULL PAPER

Preparation of buta-1,3-diynyl complexes of platinum(II) and their use in the construction of neutral molecular squares: synthesis, structural and theoretical characterisation of *cyclo*-{Pt(μ-C≡CC≡C)(dppe)}$_4$ and related chemistry

Michael I. Bruce,[a] Karine Costuas,[a,b] Jean-François Halet,[b] Ben C. Hall,[a] Paul J. Low,[a,c] Brian K. Nicholson,[d] Brian W. Skelton[e] and Allan H. White[e]

[a] *Department of Chemistry, University of Adelaide, Adelaide, South Australia 5005. E-mail: michael.bruce@adelaide.edu.au*
[b] *Laboratoire de Chimie du Solide et Inorganique Moléculaire, UMR 6511 CNRS, Université de Rennes 1, Institut de Chimie de Rennes, Avenue du Général Leclerc, 35042 Rennes cedex, France*
[c] *Department of Chemistry, University of Durham, South Road, Durham, UK DH1 3LE*
[d] *Department of Chemistry, University of Waikato, Hamilton, New Zealand*
[e] *Department of Chemistry, University of Western Australia, Crawley, Western Australia 6009*

Received 3rd September 2001, Accepted 7th November 2001
First published as an Advance Article on the web 11th January 2002

Copper(I)-catalysed reactions of *cis*-PtCl$_2$(L)$_2$ (L = PEt$_3$, L$_2$ = dppe, dppp) with buta-1,3-diyne have given the corresponding diynyl complexes, *cis*-Pt(C≡CC≡CH)$_2$(L)$_2$ (L = PEt$_3$ **1**, L$_2$ = dppe **2**, dppp **3**) whose solid-state structures have been determined from single crystal X-ray diffraction studies. Theoretical calculations were carried out to probe the electronic structure of these diynyl complexes. Complex **2** reacts with Co$_2$(CO)$_8$ to give a bis-adduct **5** and with Ru$_3$(μ-dppm)(CO)$_{10}$ to give a mono-adduct **6**; in both, the least hindered C≡C triple bond(s) is(are) coordinated. Lithiation (LiBu^t) of **2** gives a dilithio derivative, which has been converted to dimethyl **7** or mono-SiMe$_3$ **8** or -Au(PPh$_3$) **9** complexes. Cu(I) and Ag(I) (M^I) adducts (“tweezer” complexes) have been obtained from reactions of **2** with M^{I}SCN or [M^I(NCMe)$_4$]$^+$. An ES mass spectrometric study of the interactions of **2** with Group 1 cations and with Tl$^+$ is also described; comparative experiments with {W(CO)$_3$Cp}$_2$(μ-C$_8$), in which the four C≡C triple bonds do not have a “tweezer” conformation, have also been carried out. The degree of association is determined by the competitive solvation of the Group 1 cation. Coupling of the buta-1,3-diynyl complexes with Pt(OTf)$_2$(L′)$_2$ gives homo- or mixed-ligand molecular squares *cyclo*-{(L)$_2$Pt(μ-C≡CC≡C)$_2$Pt(L′)$_2$}$_2$ (L, L′ = PEt$_3$, L$_2$, L′$_2$ = dppe, dppp; not all combinations), of which the molecular structure of *cyclo*-{Pt(μ-C≡CC≡C)(dppe)}$_4$ **17** is described (as solvates containing dmso). The molecular squares form adducts with substituted ammonium triflates [NH$_2$R$_2$][OTf] (R = Et, Pr^i, Cy; NH$_2$R$_2$ = dbuH) and with Group 11 cations [M^I(NCMe)]$^+$.

Introduction

The design and synthesis of molecules having specific 2D or 3D architectures is of much current interest, such structures including molecular rods, squares, hexagons and boxes.[1,2] Assemblies of molecular squares containing transition metals by supramolecular techniques were among the first areas of success. As edges, a variety of *exo*-bidentate ligands have been employed including *N*-donor ligands such as 4,4′-bipyridyl or 2,7-diazapyrene, and more recently 4-phenyl- or 4-ethynylpyridines and 4,4′-biphenyldiyl. Stang and coworkers have reported high yield syntheses of complexes such as [{Pt(μ-4,4′-bpy)L$_2$}$_4$]$^{8+}$ (L = PEt$_3$, L$_2$ = dppp), [{Pt(μ-C$_6$H$_4$CN-4)L$_2$}$_4$]$^{4+}$ or [{Pt(μ-C≡CC$_5$H$_4$N-4)L$_2$}$_4$]$^{4+}$.[3] The challenge of making similar molecules having atomic chains as edges, such as the buta-1,3-diyne-1,4-diyl (C$_4$) ligand, has aesthetic appeal as well as a practical advantage, since the resulting complexes are neutral and may enclose larger cavities than exist in molecules in which the edges consist of aromatic or similar bulky groups. In order for 2D or 3D molecules to be built, the reactive metal sub-units need to have two or more ligands which can enter into further reactions. Some of the most extensively used metal systems of this type are the square-planar platinum(II) bis(tertiary phosphine) complexes, PtX$_2$L$_2$. Reactions of 1-alkynes with chloroplatinum(II) precursors result in the formation of *cis*- or *trans*-bis(alkynyl)platinum(II) complexes, according to the geometry of the starting material. The bis(alkynyl)platinum sub-units subtend angles of *ca.* 90 or 180° at the platinum, respectively. While the *trans* isomers have long been used to make polymeric materials containing platinum in the backbone,[4,5] the *cis* isomers are receiving increasing attention because of their ability to act as “molecular tweezers”, whereby small metal–ligand fragments can be stabilised within the bite of the two alkyne arms.[6] More recently, a series of complexes containing long poly-yne chains capped by PtR{P(tol)$_3$}$_2$ fragments (R = tol, C$_6$F$_5$) have been described.[7]

In the last few years the synthesis and properties of many buta-1,3-diyne-1,4-diyl complexes containing metals other than platinum have been reported.[8–14] These complexes have been obtained either directly from buta-1,3-diyne, or from silylated or stannylated derivatives of the diyne. Detailed studies have been carried out on {MnI(dppe)$_2$}$_2$(μ-C≡CC≡C),[9] {Re(NO)(PPh$_3$)Cp*}$_2$(μ-C≡CC≡C),[10] {Fe(dppe)Cp*}$_2$(μ-C≡CC≡C)[11] and {Ru(PPh$_3$)(PR$_3$)Cp}$_2$(μ-C≡CC≡C) (R = Ph, Me).[12] Heterometallic complexes in which two different metal centres are linked by the unsaturated carbon chain are also known.[8b,c,15] All of the systems described so far have been one-dimensional.

We have briefly described the ready synthesis of buta-1,3-diynyl complexes of platinum(II) directly from buta-1,3-diyne.[8b,c] This paper gives the full details of this chemistry,

DOI: 10.1039/b107929h

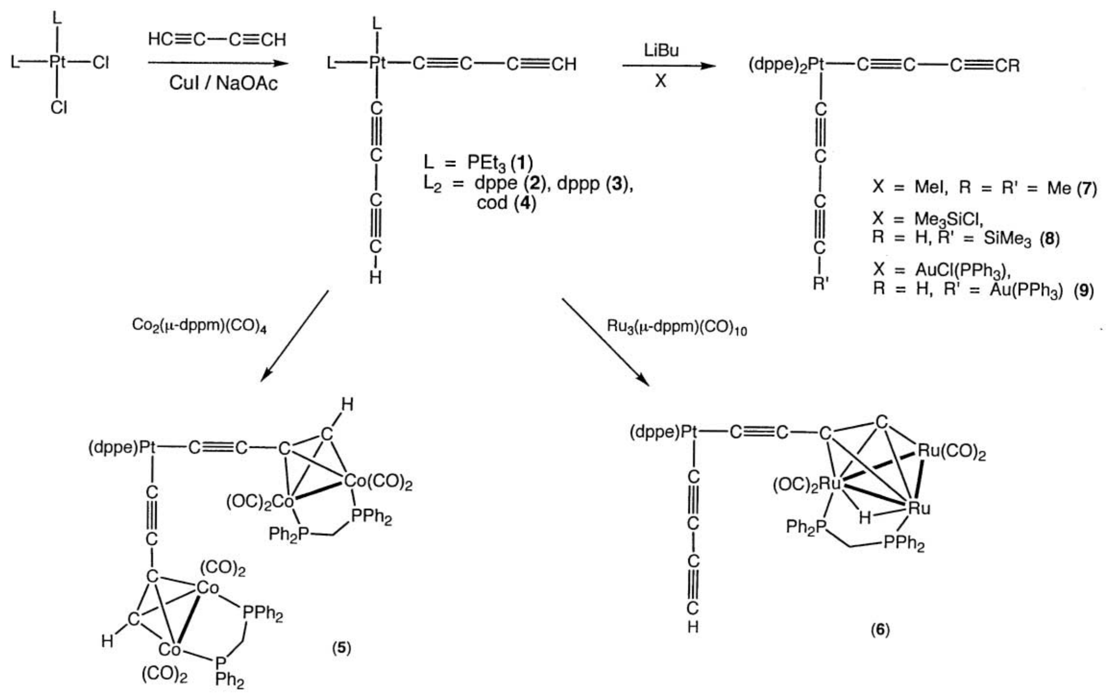

Scheme 1 Complexes **5**–**9** were obtained from Pt(C≡CC≡CH)$_2$(dppe) and the indicated reagents.

describing the preparation and structural characterisation of several molecular tweezers and their self-assembly with appropriate *cis*-Pt(OTf)$_2$(L)$_2$ (L = PEt$_3$, L$_2$ = dppe, dppp) complexes to give molecular squares. During these studies, related chemistry was published by Tessier and Youngs and their coworkers, including full structural characterisation of a molecule with C$_4$PtC$_4$ edges.[16]

Results and discussion

Preparation of *cis*-bis(diynyl)platinum(II) compounds

As previously communicated,[8b] the complexes *cis*-PtCl$_2$(L)$_2$ react with buta-1,3-diyne in dmf–diethylamine solution in the presence of CuI to give *cis*-Pt(C≡CC≡CH)$_2$(L)$_2$ (L = PEt$_3$ **1**, L$_2$ = dppe **2**, dppp **3**; Scheme 1) in high yields. These white or pale yellow complexes can be recrystallised from benzene–hexane or CH$_2$Cl$_2$–hexane mixtures and their identities have been confirmed crystallographically. Their spectroscopic properties were in accord with their solid-state structures. In the IR spectra of **1**, bands at 3249 and 2147 cm^{-1} were assigned to ν(≡CH) and ν(C≡C) absorptions respectively, while similar bands were found at 3288 and 2147 cm^{-1} for **2** and at 3296 and 2151 cm^{-1} for **3**. In the ^{1}H NMR spectra, the acetylenic protons are found at δ *ca.* 1.8 ppm and show coupling to the two chemically equivalent but magnetically non-equivalent ^{31}P nuclei. Other signals are consistent with the phosphine substituents present, with **1** showing signals arising from the ethyl groups at δ 1.08 (CH$_3$) and δ 1.97 (CH$_2$). Both **2** and **3** showed peaks corresponding to the phenyl rings at δ *ca.* 7.30–7.90, and a multiplet corresponding to the methylene protons of the phosphine backbone at δ 2.42 or δ 2.70 ppm for **2** and **3**, respectively. In the ^{13}C NMR spectra, relatively weak signals were recorded for the carbon chains at δ *ca.* 94, 80, 72 and 62. All signals were singlets with no discernible coupling to Pt or P which precluded assignments to particular carbon atoms. However, the lower field signals probably arise from C$_\gamma$ and C$_\delta$ (where C$_\alpha$, C$_\beta$, $\cdots$, *etc.*, denote the carbons of the C$_4$ chain moving out from the Pt centre). The ^{31}P NMR spectra contained the usual apparent triplets at δ 5.44 [J(PPt) = 2262 Hz] for **1**, at δ 43.26 [J(PPt) = 2288 Hz] for **2** and at δ −6.69 [J(PPt) = 2204 Hz] for **3**. These coupling constants are consistent with the *cis*-orientation of the two tertiary phosphine nuclei.[17] The electrospray (ES) mass spectra of the three complexes are similar, with addition of alkali metal or silver(I) ions resulting in the formation of ion aggregates [M + M′]$^+$ and [2M + M′]$^+$ (M′ = Na$^+$ or Ag$^+$) as the only observable ions. These observations prompted a more detailed study into the formation of the adduct ions, which is discussed further below.

A similar reaction between PtCl$_2$(cod) and the diyne afforded an unstable brown material which was not fully characterised. However, addition of one equivalent of dppe to the initial reaction mixture afforded a quantitative yield of **3**, consistent with the intermediate formation of Pt(C≡CC≡CH)$_2$(cod) **4** and subsequent replacement of the cod by the dppe ligand. This method could prove useful in the preparation of further examples not otherwise readily obtained.

Molecular structures of *cis*-Pt(C≡CC≡CH)$_2$(L)$_2$ (L = PEt$_3$ 1, L$_2$ = dppe 2, dppp 3)

Plots of a single molecule of each of the three complexes are shown in Fig. 1–3 and important structural parameters are

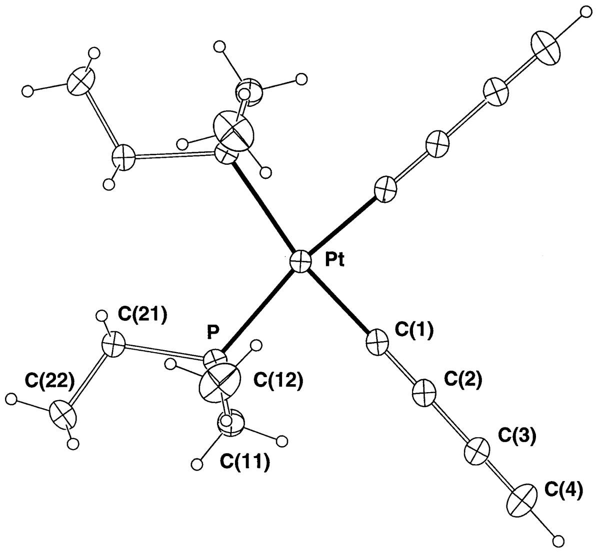

Fig. 1 Projection of *cis*-Pt(C≡CC≡CH)$_2$(PEt$_3$)$_2$ (**1**), showing atom numbering scheme.

Table 1 Selected bond parameters for butadiynyl–platinum complexes **1**, **2** and **3**

	1	**2**	**3**	dcype[16]
Pt–C(1)	1.976(4)	2.20(1)	1.997, 2.002(9)	2.03(4), 2.06(2)
C(1)–C(2)	1.218(6)	1.17(2)	1.21, 1.18(1)	1.15, 1.17(2)
C(2)–C(3)	1.390(6)	1.36(2)	1.36, 1.37(1)	1.39, 1.37(3)
C(3)–C(4)	1.174(7)	1.16(2)	1.17, 1.17(2)	1.17, 1.19(3)
Pt–P	2.319(1)	2.269(3)	2.304, 2.305(2)	2.271(8), 2.278(5)
P–C(0)	—	1.84(1)	1.83(1), 1.811(9)	1.84, 1.83(2)
C(0)–C(0′)	—	1.49(2)	1.52, 1.53(1)	1.53(3)
C(1)–Pt–C(1′)	86.5(2)	93.2(5)	88.9(3)	93.2(11)
C(1)–Pt–P	84.1(1)	90.5(3)	84.7, 89.7(3)	88.4(9), 92.8(6)
P–Pt–P′	105.22(4)	86.2(1)	97.02(8)	86.3(2)
Pt–C(1)–C(2)	179.2(4)	171.7(9)	175.2, 171.0(8)	177(3), 175(2)
C(1)–C(2)–C(3)	179.8(5)	176(1)	173.6(9), 175(1)	175, 179(2)
C(2)–C(3)–C(4)	179.7(7)	175(1)	178, 176(1)	177, 179(2)
C(1)–Pt–P	170.7(1)	173.7(3)	176.8, 170.9(3)	175.3(6), 170.6(10)
Pt–P–C(0)	—	107.2(4)	117.7, 115.6(3)	109.8(7), 108.6(6)
P–C(0)–C(0′)	—	110.0(8)	114.0, 116.7(6)	110.5(14), 113.6(12)
[P]C(1)–C(2)–C(3)	—	—	112.2(7)	

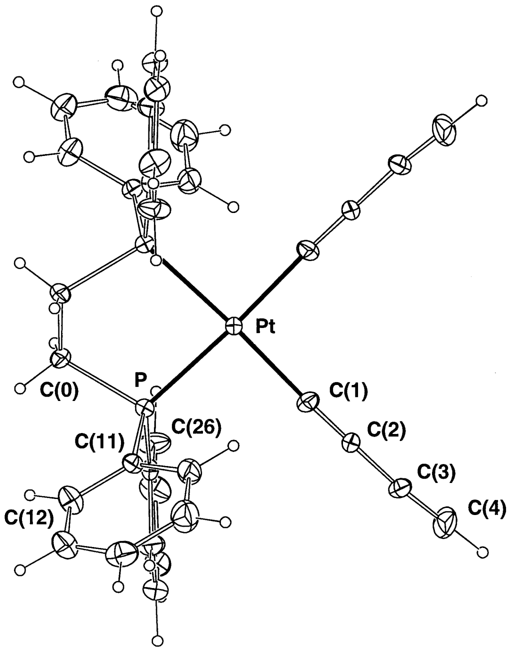

Fig. 2 Projection of Pt(C≡CC≡CH)$_2$(dppe) (**2**).

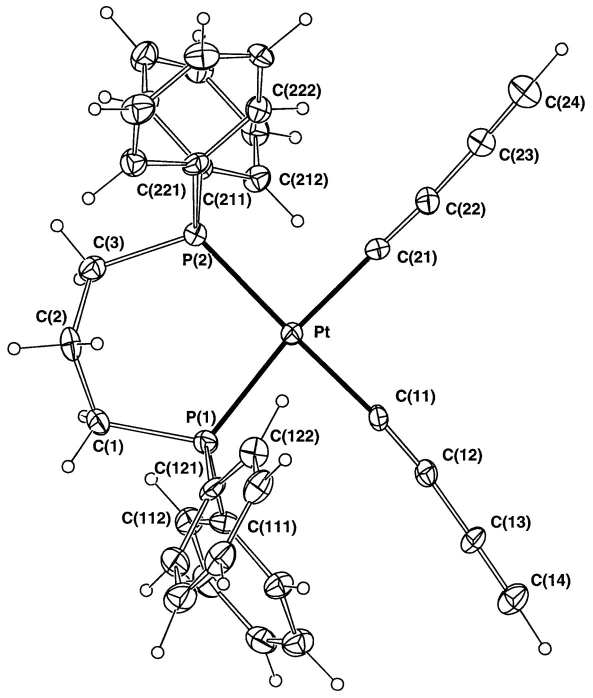

Fig. 3 Projection of Pt(C≡CC≡CH)$_2$(dppe) (**3**).

collected in Table 1. Some comparable bond parameters for Pt(C≡CC≡CH)$_2$(dcype) [dcype = 1,2-bis(dicyclohexylphosphino)ethane] are also listed.[16] In **1**, the molecule lies with the metal on a site of *mm* symmetry, so that only one quarter, containing half a ligand of each type, comprises the asymmetric unit of the structure. In **2**, the molecule is also disposed thus, the axis passing through the mid-point of the central C–C bond of the diphosphine ligand. Bond parameters are similar for all complexes. The platinum atom has approximate square-planar coordination, the bulk of the PEt$_3$ ligands in **1** being associated with expanded P–Pt–P angles (105.22(4)°), whereas the angles subtended at Pt in the chelate complexes are dependent on the bite-angles of the chelating phosphines. Thus, we find values for P(1)–Pt–P(2) of 86.2(1) and 97.02(8)° for **2** and **3** respectively. There are similar variations in the C–Pt–C angles [86.5(2), 93.2(5) and 88.9(3)° for **1**, **2** and **3** respectively] while the P–Pt–C angles vary between 84.1(1) and 90.5(3)°.

The Pt–P distances are 2.319(1) **1**, 2.269(3) **2** and 2.304, 2.305(2) Å **3**, which may be compared with values of 2.220(8) Å for PtCl$_2$(dppe)[18] and 2.233(1), 2.2317(8) Å for PtCl$_2$(dppp).[19] The Pt–C distances are 1.976(4) **1**, 2.02(1) **2** and 1.997, 2.002(9) Å **3** [*cf.* Pt–C 2.10, 2.04(1) Å in *cis*-Pt(C≡CPh)$_2$(PPh$_3$)$_2$[20]]. Along the C$_4$ chain from the metal, alternate short and long C–C separations of 1.218, 1.390 and 1.174(6) Å (for **1**), 1.17, 1.36 and 1.16(2) Å (for **2**) and 1.21, 1.36, 1.17(1) Å (for **3**) confirm retention of diynyl character along the C$_4$ chain. The diynyl H atoms were not refined. In **1**, angles at the carbon atoms of the chain range between 179.2(4) and 179.7(7)°, *i.e.* the C$_4$ chains are linear within experimental error. In contrast, the C$_4$ chains are distinctly non-linear in **2** and **3** with the corresponding angles ranging from 171.7(9) to 176(1)° (for **2**) and 171.0(8) to 178(1)° (for **3**); the largest departures from linearity are found at atoms C(1) and C(2). In **3** the C(1)–Pt–C(1′) and P–Pt–P′ angles are 88.9(3) and 97.02(8)°, respectively, perhaps the result of steric interactions between the phenyl groups of the tertiary phosphine ligands and the C$_4$ chains (but see also the theoretical discussion below). The facile bending of C$_n$ chains has been recently noted and discussed in a series of complexes containing longer C$_n$ chains (n = 6–12) attached to rhenium[21] or platinum.[7] In this context, it is of interest to note the size of the anisotropic displacement parameters of C(4), which are nearly twice those for the other three carbon atoms of the chain. It is evident that deformation of the C$_4$ chain is a low energy process. Intramolecularly, we note that in **3** C(22) ··· H(222) (2.6$_2$ Å) is especially close, while Pt ··· H(16)

(2.9$_8$ Å) in **2** and Pt ··· H(122, 212) (2.8$_2$, 3.0$_5$ Å) in **3** may be considered quasi-agostic.

Theoretical considerations

Compounds **1**, **2** and **3** are typical 16-electron square-planar $ML_2L'_2$ complexes. Extended Hückel (EH) and Density Functional (DF) molecular orbital calculations were carried out on the hydrogen-substituted model complex Pt(C≡CC≡CH)$_2$(dHpe) (**2-H**) and derivatives in order to gain further insight into the electronic structure of these 16-electron platinum(II) diynyl species. Computational details are given in the Experimental section.

A simple EH molecular orbital diagram (Fig. 4) is useful for qualitatively understanding the bonding between the C_4H chains and the metallic fragment. Using a fragment analysis, the formation of **2-H** of C_{2v} symmetry can be envisioned as the result of the interaction of the frontier molecular orbitals (FMO) associated with the two $(C_4H)^-$ units with those of the ML_2 platinum fragment $[Pt(dHpe)]^{2+}$. The charges on the fragments have been arbitrarily chosen in such a way that the number of electrons associated with the carbon atoms of the C_4H fragments is consistent with the octet rule.

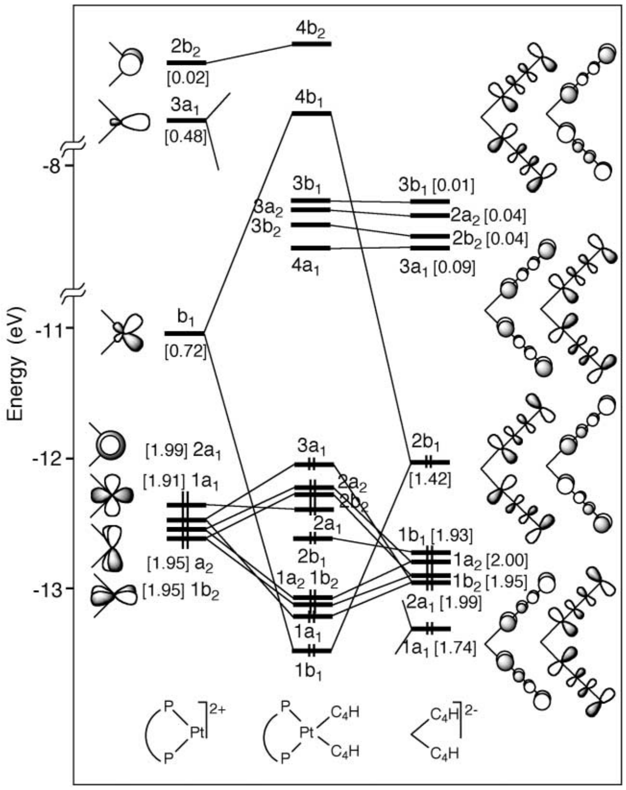

Fig. 4 EH orbital interaction diagram for the model complex Pt(C≡CC≡CH)$_2$(dHpe) (**2-H**) of C_{2v} symmetry. FMO occupancies after interaction are given in brackets. For clarity the C_4H σ-type FMOs la$_1$ and 2b$_1$ are not sketched.

The non-conical C_{2v} $[Pt(dHpe)]^{2+}$ metal fragment possesses four mainly d-based orbitals at low energy (1b$_2$, a$_2$, 1a$_1$, and 2a$_1$), separated from two high-lying hybrid orbitals, one radial (3a$_1$) and one tangential (b$_1$), which point away from the dHpe ligand. At higher energy lies a metal p orbital, 2b$_2$.[22] Such a fragment is set up to interact with the FMOs of the two $(C_4H)^-$ units, restoring the usual splitting pattern for a square-planar d^8 ML_4 complex. The FMOs of the two $(C_4H)^-$ units consist of a set of in-phase and out-of-phase combinations of σ, π and π* carbon orbitals (see the right-hand side of Fig. 4). The Pt–C bonding in **2-H** is dominated by strong σ-type interactions between the vacant hybrid metal orbitals 3a$_1$ and b$_1$ and the in-phase and out-of-phase combinations of the C_4H σ-type FMOs 1a$_1$ and 2b$_1$, respectively (see Fig. 4). This leads to an important electron donation from the C_4H units towards the metallic fragments as illustrated numerically by the braced digits in Fig. 4 which indicate the electron occupation of FMOs following the interaction of the component fragments.

An interesting point to discuss is the additional interaction of the π/π* orbitals of the C_4H ligands with the metal fragment. The large energy difference between the donor metallic FMOs and the four low-lying acceptor π* orbitals on the C_4H entities limits the degree to which back-bonding interactions may contribute to the M–C bonding in **2-H**. The electron occupation of the acceptor carbon orbitals is computed to be only between 0.01 and 0.09. It turns out that the major Pt–C π-type interactions are filled/filled interactions between the occupied carbon and metal π orbitals. Among the four π FMOs of the C_4H ligands, three of them, the in-plane 2a$_1$, and the out-of-plane 1b$_2$ and 1a$_2$ FMOs interact rather strongly with the corresponding occupied metallic FMOs 1b$_2$, a$_2$ and 1a$_1$. As a result of these interactions, the C_4H π orbitals are stabilised, whereas the metallic orbitals are somewhat destabilised and become the HOMOs of **2-H**. An important consequence of these π-type interactions is the strong mixing of the C_4H and Pt(dHpe) FMOs which leads to a large percentage contribution from the carbon atoms of the C_4H unit to the HOMOs of **2-H** (54, 57 and 61% platinum and 46, 43 and 39% C_4H character for the 3a$_1$, 2a$_2$ and 2b$_2$ MOs, respectively). The HOMOs are therefore delocalised over the entire Pt$(C_4H)_2$ core, being antibonding between Pt and C(1) and between C(2) and C(3), but bonding between C(1) and C(2) and between C(3) and C(4). It may be concluded that any eventual oxidation process which would involve loss of electrons from these HOMOs will affect the whole molecule. A large gap of 3.18 eV is computed between the 3a$_1$ HOMO and the 4a$_1$ LUMO which nearly exclusively derives from one C_4H π* component.

These qualitative conclusions are further supported by density functional molecular orbital calculations, which were carried out on different Pt(C≡CC≡CH)$_2$(L)$_2$ species. For instance, calculations on the geometry-optimised hydrogen-substituted model complex Pt(C≡CC≡CH)$_2$(dHpp) (**3-H**) shows a HOMO/LUMO gap of 3.07 eV with HOMOs largely delocalised both on the metal centre and the diynyl chains. With computed Pt–C distances of 1.977, 1.976 Å, Pt–P distances of 2.259 Å, C(1)–C(2), C(2)–C(3) and C(3)–C(4) separations of 1.231, 1.364 and 1.221 Å, respectively, and C–Pt–C and P–Pt–P angles of 93.2° and 95.5°, respectively, the optimised geometry of **3-H** compares rather well with that of the crystallographically characterised complex Pt(C≡CC≡CH)$_2$(dppp) (**3**) (see Table 1). Interestingly enough, the PtCCCCH sequences are not strictly linear but are slightly curved [Pt–C(1)–C(2) 172.6, 172.9, C(1)–C(2)–C(3) 176.6, 177.9, and C(2)–C(3)–C(4) 178.9, 177.9°]. Nevertheless the curvature is slightly greater in the experimental complex **3** (see Table 1), suggesting that the bending of the C_4 chains implicates both electronic effects (correlated with geometrical parameters) and crystal packing forces. It is noteworthy that the most bent carbon chains are observed with the smallest bite P–Pt–P′ angles (see Table 1).

EH Mulliken and DF Hirshfeld[23] atomic net charges are the following: −0.18, 0.09 for Pt, −0.41, 0.64, 0.21 for P, −0.19 for C(1), −0.05, −0.07 for C(2), 0.06, −0.03 for C(3) and −0.23, −0.11 for C(4). They indicate some flow of electron density from the phosphorus and, to a lesser extent, the metal atoms to part of the carbon chains. It follows that a substantial amount of negative charge resides on C(1) and to a lesser extent on C(4), whereas C(2) and C(3) remain nearly neutral.

Reactions of 2 with $Co_2(CO)_8$ or $Co_2(\mu\text{-dppm})(CO)_6$

The cobalt complexes $Co_2(CO)_8$ and $Co_2(\mu\text{-dppm})(CO)_6$ have been used as protecting groups for alkynes[24] as well as to confirm the presence of extended C_n chains in poly-yne complexes.[25] Reactions between $Co_2(CO)_8$ and $Pt(C\equiv CC\equiv CH)_2(dppe)$ resulted in the formation of many products in low yield, none of which were satisfactorily characterised. However, reaction of **2** with two equivalents of $Co_2(\mu\text{-dppm})(CO)_6$ resulted in the formation of red $Pt\{C\equiv CC_2H[Co_2(\mu\text{-dppm})(CO)_4]\}_2(dppe)$ **5** in 50% yield. Coordination of the Co_2 fragments to both C_4 arms was established by IR, NMR and ES mass spectrometry and confirmed by a (relatively imprecise) single-crystal X-ray structure determination. The IR spectrum contained three peaks at 2016 [ν(C≡C)], 1990 and 1960 cm^{-1} [ν(CO)]. The ^{31}P NMR spectrum has two resonances, a triplet at δ 34.96 [J(PPt) = 2258 Hz] (dppe) and a singlet at δ 20.66 (dppm). The negative-ion ES mass spectrum contained a molecular anion at *m/z* 1920, which fragmented by successive loss of up to eight CO groups. The positive-ion spectrum of a solution containing NaOMe has a single peak at *m/z* 1943, corresponding to the $[M + Na]^+$ ion. A molecule of **5** is shown in Fig. 5, with the important bond lengths and angles being summarised in Table 2. While detailed comparisons with the structure of **2** are not warranted, the structure determination clearly shows that the two Co_2 moieties are attached to the least sterically hindered C≡C triple bonds of each C_4 arm. The usual bending back of the substituents on this C_2 unit is found.

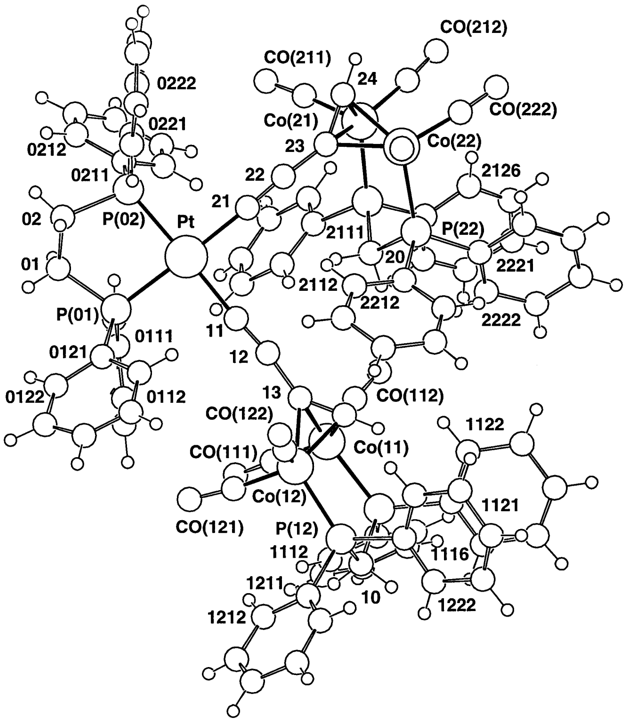

Fig. 5 Projection of $Pt\{C\equiv CC_2H[Co_2(\mu\text{-dppm})(CO)_4]\}_2(dppe)$ (**5**).

Table 2 Selected bond parameters for $Pt\{C\equiv CC_2H[Co_2(\mu\text{-dppm})(CO)_4]\}_2(dppe)$ (**5**)

Pt–P(01)	2.272(8)	Co(11)–P(11)	2.197(8)
Pt–P(02)	2.251(8)	Co(12)–P(12)	2.215(8)
Pt–C(11)	2.03(3)	Co(22)–P(22)	2.212(9)
Pt–C(21)	2.01(3)	Co(24)–P(22)	2.217(8)
C(11)–C(12)	1.20(4)	Co(11)–C(13)	1.89(3)
C(12)–C(13)	1.43(4)	Co(11)–C(14)	1.87(3)
C(13)–C(14)	1.25(4)	Co(12)–C(13)	1.95(3)
C(21)–C(22)	1.22(4)	Co(12)–C(14)	1.91(3)
C(22)–C(23)	1.38(4)	Co(21)–C(23)	1.98(2)
C(23)–C(24)	1.32(3)	Co(21)–C(24)	2.02(3)
Co(11)–Co(12)	2.458(5)	Co(22)–C(23)	1.98(3)
Co(21)–Co(22)	2.472(5)	Co(22)–C(24)	2.02(3)
P(01)–Pt–P(02)	86.0(3)	Pt–C(11)–C(12)	176(2)
C(11)–Pt–C(21)	90(1)	C(11)–C(12)–C(13)	173(3)
P(01)–Pt–C(11)	91.4(8)	C(12)–C(13)–C(14)	142(3)
P(01)–Pt–C(21)	176.1(7)	Pt–C(21)–C(22)	173(2)
P(02)–Pt–C(11)	175.8(8)	C(21)–C(22)–C(23)	173(3)
P(02)–Pt–C(21)	92.2(8)	C(22)–C(23)–C(24)	144(3)

Reaction of 2 with $Ru_3(\mu\text{-dppm})(CO)_{10}$

In a manner analogous to the reactions of organic 1-alkynes[26] and other terminal diynyl complexes,[27] facile oxidative addition of **2** to $Ru_3(\mu\text{-dppm})(CO)_{10}$ gave yellow $Ru_3(\mu\text{-H})\{\mu_3\text{-}\eta^2\text{-}C_2C\equiv C\text{-}[Pt(C\equiv CC\equiv CH)(dppe)]\}(\mu\text{-dppm})(CO)_7$ **6** in high yield. The composition was determined by microanalysis, NMR and ES mass spectrometry and showed that only one Ru_3 cluster is present, presumably for steric reasons. A doublet hydride resonance at δ −19.39 [J(HP) = 34 Hz] is similar to that found for $Ru_3(\mu\text{-H})\{\mu_3\text{-}\eta^2\text{-}C_2C\equiv C[W(CO)_3Cp]\}(\mu\text{-dppm})(CO)_7$.[27] The negative ion ES mass spectrum of **6** with added NaOMe contained $[M + OMe]^-$ (*m/z* 1607) and $[M - H]^-$ (*m/z* 1575) with further fragmentation occurring by loss of CO ligands.

Lithiation reactions

When **2** is treated with two equivalents of $LiBu^t$ at −78 °C an orange solution is formed which is assumed to contain the dilithio intermediate $Pt(C\equiv CC\equiv CLi)_2(dppe)$, since addition of two equivalents of iodomethane resulted in the formation of the dimethyl derivative $Pt(C\equiv CC\equiv CMe)_2(dppe)$ **7** in 93% yield. This compound was characterised by NMR and ES mass spectrometry. The ^1H and ^{13}C NMR spectra showed the presence of equivalent Me groups (δ_H 1.28, δ_C 50.76). The ES mass spectrum contained two peaks, the molecular ion at *m/z* 719 and $[M + Li]^+$ at *m/z* 726.

Treatment of the dilithio derivative with $SiClMe_3$ resulted in the formation of the monosilylated complex, $Pt(C\equiv CC\equiv CH)(C\equiv CC\equiv CSiMe_3)(dppe)$ **8** (68%). The IR spectrum contained two ν(C≡C) bands at 2149 and 2089 cm^{-1}, while the ^1H and ^{13}C NMR spectra both confirmed the presence of the $SiMe_3$ group (δ_H 0.07, δ_C 1.30). Monoauration similarly occurs in the reaction between the dilithio derivative and $AuCl(PPh_3)$ to give $Pt(C\equiv CC\equiv CH)\{C\equiv CC\equiv C[Au(PPh_3)]\}(dppe)$ **9** in 60% yield. This was identified by IR [two ν(C≡C) bands at 2140 and 2084 cm^{-1}] and ^1H NMR spectrometry (δ 1.22 for ≡C*H*). Integration of the aromatic region confirmed that only one $Au(PPh_3)$ group was present. The ES mass spectrum contained M^+ (*m/z* 1149). Complex **9** was also obtained by treating **2** with $AuCl(PPh_3)$ in the presence of CuCl as catalyst. Molecular modelling of $Pt\{C\equiv CC\equiv C[Au(PPh_3)]\}_2(dppe)$ showed no steric interactions between phenyl groups and it is not yet apparent why only the mono-substituted derivatives **8** and **9** could be isolated.

cis-Bis(buta-1,3-diynyl)platinum(II) complexes as molecular tweezers

Many examples of *cis*-bis(alkynyl)metal complexes acting as chelating ligands ("molecular tweezers") towards metal fragments have been reported,[6] among which examples with guest fragments M^IX (M^I = Cu, Ag) feature prominently.[28] When either CuSCN or AgSCN is added to **2**, mono-adducts $M^I(SCN)\{(HC\equiv CC_2)_2Pt(dppe)\}$ (M^I = Cu **10**, Ag **11**, respectively; Scheme 2) are formed in excellent yields. The silver derivative is light sensitive, decomposing rapidly under standard laboratory fluorescent lights. Evidence for their composition was obtained from IR, NMR and mass spectrometry, together with elemental analyses. The IR spectra of **10** and **11** showed ν(CN) at *ca.* 2155 cm^{-1} from the SCN group and ν(C≡C) bands at lower frequencies than that of **2** (2098 **10** and 2093 cm^{-1} **11**). This is in agreement with the back-bonding from the M^I centre to the alkyne. While the ^1H NMR spectrum showed little change from that of **2**, the ^{13}C NMR spectrum showed a downfield shift of C_α and C_β as a result of their complexation. The ES mass spectra were similar with M^+ at *m/z* 755 for **10** and *m/z* 799 for **11**. Also present were peaks corresponding to $[2(\mathbf{2}) + M^I]^+$ at *m/z* 1446 (**10**) or 1491 (**11**). Presently no X-ray structural

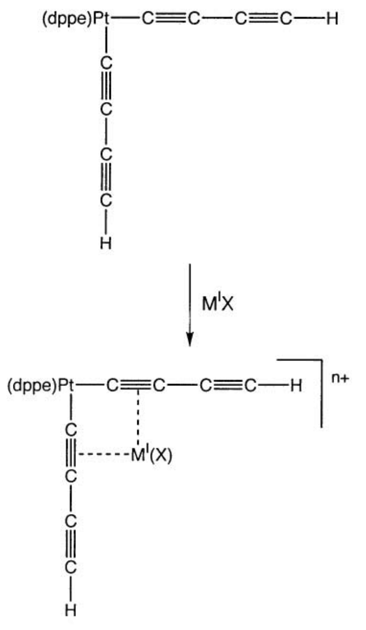

M^I = Cu, X = SCN, n = 0 (**10**)
M^I = Ag, X = SCN, n = 0 (**11**)
M^I = Cu, X = NCMe, n = 1 (**12**)
M^I = Ag, X = NCMe, n = 1 (**13**)

Scheme 2

information is available for either complex, but it is likely that they have structures similar to those found for related complexes[28] in which the M^I centre has approximate trigonal-planar coordination from the two η^2-alkyne groups and the η^1-SCN ligand, although the $M^I(C_2)_2Pt$ system is non-planar.

Addition of $[M^I(NCMe)_4]BF_4$ to **2** similarly gives complexes of composition $[M^I(NCMe)\{(HC{\equiv}CC_2)_2Pt(dppe)\}]BF_4$ (M^I = Cu **12**, Ag **13**) in high yields. Their IR spectra are similar with ν(≡CH) and ν(C≡C) bands at 3255 and 2141 cm^{-1} (for **12**) and 3281 and 2139 cm^{-1} (for **13**), both spectra also containing broad ν(BF) absorptions at 1060 cm^{-1}. The ^1H NMR spectra showed very little difference from that of **2** with the exception of signals arising from the coordinated MeCN at δ 2.00. The ^{13}C NMR spectra showed a downfield shift of the C_α and C_β resonances as a result of attachment of the $[M^I(NCMe)]^+$ fragment. The ES mass spectra showed similar features with $[\mathbf{2} + M^I(NCMe)]^+$ at *m*/*z* 796 for **12** and 840 for **13**. Also present were peaks corresponding to $[2(\mathbf{2}) + M^I]^+$ at *m*/*z* 1446 (**12**) and 1491 (**13**).

While treatment of **12** with one equivalent of $[Ag(NCMe)_4]^+$ resulted in the appearance of a peak corresponding to $[\mathbf{3} + Ag]^+$ at *m*/*z* 799, there was no change observed in the spectrum of a solution of **13** with $[Cu(NCMe)_4]^+$. These qualitative results indicate that the silver is more strongly held than the copper and prompted us to attempt to obtain more information concerning the formation of adducts of these molecular tweezers with mono-positive cations of Groups 1 and 11. We have carried out a survey of the ES mass spectra of solutions containing these complexes with added cations.

Electrospray mass spectrometry of bis(diynyl)platinum(II) complexes

It is now generally accepted that the technique of ES mass spectrometry is a reliable way of determining which ionic species are present in a solution, since the gentle ionisation process transfers ions intact to the gas phase for analysis in the mass spectrometer. As a consequence, several ES mass spectrometry studies have investigated semi-quantitatively the interaction of ions with complexing ligands.[29] The area has been reviewed[30] and more recent examples include the relative binding of Group 1 ions by cholic acid derivatives[31] and the complexation of metal ions by crown ethers and related ligands,[32–34] by cryptands or by valinomycin.[35] The use of metal ions, particularly Ag^+, to form ions from neutral species for analysis by ES mass spectrometry is now well established for substrates with π-electron density and for metal carbonyls.[36–39]

The availability of complexes containing polyalkyne units arranged in different ways provided interesting substrates for investigating possible interactions with metal ions, ES mass spectrometry being used to screen varying combinations rapidly and on a small scale. As noted, the ES mass spectrum of a methanolic solution of **3** containing Ag^+ ions showed clean peaks at *m*/*z* 813 and 1519, corresponding to $[\mathbf{3} + Ag]^+$ and $[2(\mathbf{3}) + Ag]^+$, respectively. Similar results were obtained in EtOH, while in MeCN ions $[\mathbf{3} + Ag(MeCN)]^+$ dominated at lower cone voltages, with increasing amounts of $[\mathbf{3} + Ag]^+$ as the cone voltage was raised. When the same complex in MeOH was treated with Li^+ ions, there was a strong ion corresponding to $[\mathbf{3} + Li + MeOH]^+$ (*m*/*z* 744) and a weaker signal from $[2(\mathbf{3}) + Li]^+$ (*m*/*z* 1418) at a cone voltage of 20 V. At 40 V, the ion $[\mathbf{3} + Li]^+$ (*m*/*z* 712) is dominant while at 80 V the ion at *m*/*z* 744 has vanished. The relative intensity of the *m*/*z* 1418 signal remains roughly constant as the cone voltage changes. With the larger cations Na^+, K^+, Rb^+, Cs^+ and Tl^+ (M′) the spectra are simpler, giving mainly ions of the type $[\mathbf{3} + M']^+$, with no solvated equivalents even at low cone voltages, together with weaker $[2(\mathbf{3}) + M']^+$ species.

To gauge the selectivity towards different ions, a solution of **3** was treated with an equimolar mixture of the mono-charged cations as their chlorides in MeOH solution. The resulting mass spectrum recorded with a cone voltage of 30 V is shown in Fig. 6, and shows selectivity in the order $Cs^+ > Tl^+ > Rb^+ > K^+ > Na^+ > Li^+$. At first sight, this seems counter-intuitive since it might have been expected that the more polarising cations would form stronger adducts with the alkyne groups on the metal complex. Taken in isolation, the stability of cation-π interactions is normally found to lie in the order $Li^+ > Na^+ > K^+$, *etc.*,[38] the reverse of the trend found and illustrated in Fig. 6. However the observed order in the present study is understandable in terms of competition between the alkyne groups and the solvent molecules for sites about the M^+ ions. Li^+ is strongly solvated by MeOH so the alkyne group would compete poorly giving weak adducts, whereas for the larger cations such as Cs^+, the MeOH molecules would be more readily displaced. Alternatively, it can be rationalised in terms of hard–soft acid–base theory; the alkyne group is a soft base

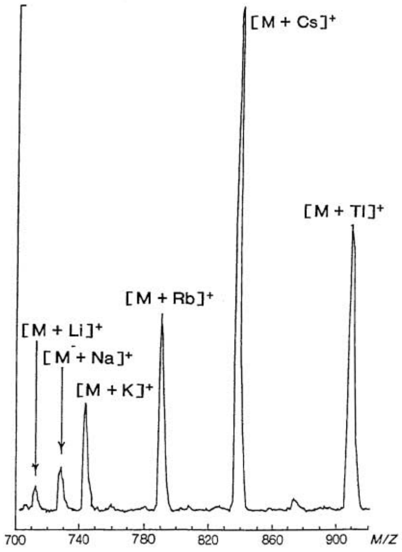

Fig. 6 The ES mass spectrum of $Pt(C{\equiv}CC{\equiv}CH)_2(dppe)$ (**3**) in MeOH in the presence of equimolar concentrations of Li^+, Na^+, K^+, Rb^+, Cs^+ and Tl^+ ions. Cone voltage was set at 30 V to minimise overlap of the $[M + Li + MeOH]^+$ signal with that of $[M + K]^+$, both at *m*/*z* 744.

while MeOH is hard, so the adduct with **3** would be most favoured for the softest acid, *i.e.* the larger cation. Not unexpectedly, none of these Group 1 cations competes effectively with Ag^+ for adduct formation. Note that the observed selectivity is not a size-based one related to a "tweezer" effect, since similar results were found for polyalkyne complexes where no tweezer effect is possible (see below).

In MeCN solutions containing the same mixture of cations, **3** gave a similar spectrum to that in Fig. 6 except that the relative intensities of the Tl^+ and Rb^+ adducts were reversed and the Li^+ adduct was barely detectable, *i.e.* $Cs^+ > Rb^+ > Tl^+ > K^+ > Na^+ \gg Li^+ \approx 0$. These differences presumably reflect the strengths of solvation of the cations in MeOH and MeCN, respectively.

Adducts of **3** with more complex mono-charged cations can also be obtained. Thus when a mixture of **3** and PhHg(OAc) in MeOH was introduced to the mass spectrometer, a signal at *m*/*z* 984 appeared and was readily assigned to the $[\mathbf{3} + HgPh]^+$ ion. The use of $[HgMe]^+$ to derivatise neutral nitrogen bases has been reported previously,[40] but we are not aware of other examples involving an HgR^+-π type complexation.

More highly charged ions, such as Ba^{2+}, Cd^{2+}, Sn^{2+}, Pb^{2+} or Hg^{2+} (added as their nitrates) do not give simple adducts with **3**. Presumably these more highly charged cations are too strongly solvated to become attached to the alkyne groups of **3**. Only with added Cu^{2+} were identifiable species recorded, but these were of the type $[\mathbf{3} + Cu]^+$ and $[2(\mathbf{3}) + Cu]^+$, arising from *in situ* reduction of Cu(II) to Cu(I). When **3** was treated with a mixture of Cu^{2+} and 1,10-phenanthroline a very strong, clean signal corresponding to $[\mathbf{3} + Cu(phen)]^+$ was found at *m*/*z* 949.

The ES mass spectra of $Pt\{C{\equiv}CC{\equiv}C[W(CO)_3Cp]\}_2(dppe)$ **14**,[8c] obtained from solutions in MeCN containing formic acid, contained an $[M + H]^+$ ion at *m*/*z* 1357, while an ion at *m*/*z* 1342 is formulated as $[2(\mathbf{14}) + 2H - CO]^{2+}$. The use of MeCN solutions containing $AgNO_3$ resulted in the formation of doubly-charged aggregate ions with masses and isotopic distributions consistent with the formulations $[\{\mathbf{14} + Ag\}_2 + 5MeCN]^{2+}$ (*m*/*z* 1566) and $[\{\mathbf{14} + Ag\}_2]^{2+}$ (*m*/*z* 1464). The complex $Pt\{C{\equiv}CC{\equiv}C[W(CO)_3Cp]\}_2(dppp)$[8c] ($\equiv M^W$) was also examined in MeOH and EtOH, although solubility was very limited. This also provided $[M^W + M']^+$ signals for $M' = Li^+$, Na^+, K^+ and Cs^+. More interestingly, with Ag^+ ions the dominant signal at *m*/*z* 1478 could be assigned to a $[\{M^W + Ag\}_2]^{2+}$ species, since the interpeak spacing in the isotope pattern was 0.5 amu. *In vitro*, coordination of two C≡C triple bonds of alkynyl-metal complexes to Cu^+ or Ag^+ ions has been found on many occasions.[41] In the present case, similar structures can be proposed in which C≡C triple bonds from two molecules of the complex effectively sandwich the Group 11 cations, rather than acting in the tweezer mode.

To determine whether **3**, with its four C≡C triple bonds, is acting in a tweezer fashion, analogous experiments were carried out with the complex $\{W(CO)_3Cp\}_2\{\mu\text{-}(C{\equiv}C)_4\}$ **15**.[42] This has the same number of alkyne groups, but they are arranged in linear fashion so that they cannot exert a tweezer effect. The results were similar. With Li^+ ions in MeOH, **15** gave signals assigned to $[\mathbf{15} + Li]^+$, $[\mathbf{15} + Li + MeOH]^+$ and $[\mathbf{15} + Li + 2MeOH]^+$ at a cone voltage of 30 V, while Na^+ gave the corresponding $[\mathbf{15} + Na]^+$ together with a weak $[\mathbf{15} + Na + MeOH]^+$. The other cations Ag^+, K^+, Rb^+, Cs^+ and Tl^+ gave ions $[\mathbf{15} + \text{cation}]^+$ only, with no solvated equivalents even at low cone voltages. However, when $[Cu(MeCN)_4][BF_4]$ was added to a MeOH solution of **15**, the major ion was $[\mathbf{15} + Cu(MeCN)]^+$. These observations are entirely consistent with competition of the cations between solvent and alkyne groups discussed earlier.

When a solution of **15** was treated with the equimolar mixture of cations, the relative intensities of the signals were $Cs^+ > Tl^+ > Rb^+ > K^+ > Na^+ > Li^+ \approx 0$. This is very similar to the distribution shown in Fig. 6 for **3**, except that negligible amounts of the Li^+ adduct were formed for **15** in competition with the other cations. This also suggests that the selectivity arises through competition with solvation, rather than by a size-dependent tweezer effect. Of interest is the observation that the spectrum of **15** in MeOH without added cations gave rise to peaks assigned to M^+ and $[M - nCO]^+$ ($n = 1, 2, 3, 4$, depending on cone voltage) arising from oxidation to the radical cation in the mass spectrometer. While this is not unknown for electron-rich species, it is a relatively rare type of ionisation under normal electrospray conditions,[36a,43,44] and no similar signals were found for **3**.

In a separate competition experiment, MeOH solutions containing equal amounts of **3** and **15** together with the Group 1 cations were examined to assess the relative ease of adduct formation. With Cs^+, the $[\mathbf{3} + Cs]^+$ signal was about three times as intense as that of $[\mathbf{15} + Cs]^+$, while for the other cations (Tl^+, Rb^+, K^+, Na^+ and Li^+) the adducts formed by **15** were barely detectable relative to the very strong $[\mathbf{3} + M']^+$ ions. This shows that the platinum complex with two orthogonal C_4H groups attaches to the cations more strongly than the tungsten example with a linear C_8 unit. This may be due to a small tweezer effect, but other explanations such as the effect of the more extended delocalised π-cloud for the C_8 ligand compared with those of two shorter C_4H groups can also be proposed.

The general pattern that is found for these complexes is that the strongest adducts form for the Group 11 cations Ag^+ and Cu^+, as would be expected for complexes involving π-interactions. With the Group 1 cations, where non-covalent (electrostatic) forces are proposed, the most abundant adducts are with the least strongly solvated cation Cs^+, where the weakly coordinating alkyne groups can most readily displace solvent molecules. This also explains the lack of ions involving association with multiply-charged ions where solvation by MeOH would be even stronger. This is in direct contrast to the ES mass spectral work referred to above where complexation of the ions by crown ethers and other *O*- or *N*-donor ligands is involved. Stronger adducts were formed with the more polarising cations and 2^+ cations gave identifiable adducts. The similarity of results for tweezer-type substrates and linear ones suggests that there is no size-related tweezer effect with the Group 1 cations.

It is also clear that in choosing cations for derivatising neutral substrates for ES mass spectral studies, the nature of the substrate directs the choice. Where the functional groups are hard, with N or O donor atoms for example, then smaller cations such as Li^+ are preferred, while for soft functional groups, especially those with π-electrons, softer cations such as Ag^+ or Cu^+ respond better.

Construction of molecular squares

The availability of the *cis*-bis(buta-1,3-diyn-1-yl) complexes **1**, **2** and **3**, which could be considered to form the two edges and corner of a square or rectangle suggested their incorporation into square molecules. However, addition of **1**, **2**, or **3** to $PtCl_2(L)_2$ under copper(I)-catalysed coupling conditions resulted in the formation of polymers, probably due to the rapid rates of these reactions, while the reaction of $Pt(OTf)_2(L)_2$ with **1**, **2** or **3** in a methanol–dichloromethane mixture resulted in rapid decomposition, probably as a result of the formation of triflic acid as a by-product of the coupling reaction. However, we were encouraged by the appearance of ions corresponding to the molecular squares in the ES mass spectra of the reaction mixtures. Accordingly, use of high dilution techniques in reactions carried out in the presence of a weak base, such as sodium acetate, resulted in the quantitative self-assembly of the molecular squares *cyclo*-$\{Pt(\mu\text{-}C{\equiv}CC{\equiv}C)(L)_2\}_4$ (Scheme 3), with little decomposition or polymer formation. Isolation of the products was achieved by evaporation to small volume, followed by addition of hexane. Cream precipitates were identified as *cyclo*-{Pt(μ-C≡CC≡C)(PEt_3)$_2$}$_4$ **16**, *cyclo*-{Pt(μ-C≡CC≡C)(dppe)}$_4$ **17** and *cyclo*-{Pt(μ-C≡CC≡C)(dppp)}$_4$ **18** (Scheme 3).

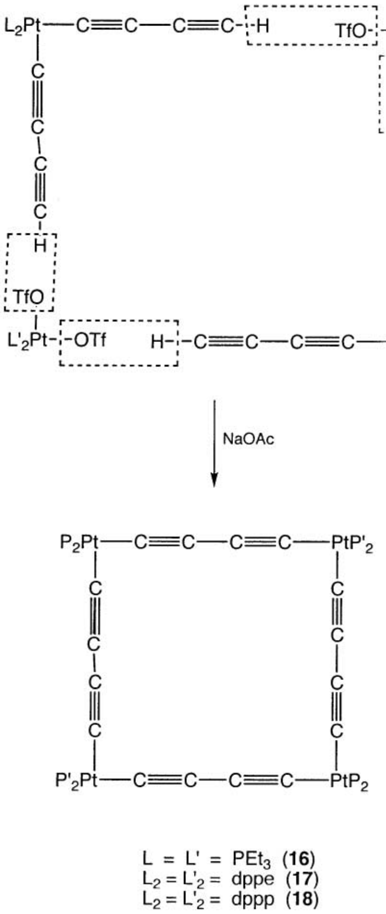

Scheme 3

The IR spectra of **16**, **17** and **18** each contained a single *ν*(C≡C) absorption at *ca.* 2145 cm^{-1}, while the ^{1}H and ^{13}C NMR spectra contained signals appropriate for the various tertiary phosphine ligands. Only in the case of **18** could the two chemically distinct carbons of the C_4 bridge be observed in the ^{13}C NMR spectrum, at δ 92.23 and 110.39, but neither *J*(CP) nor *J*(CPt) could be resolved. The ^{31}P NMR spectra each contained triplet resonances [*J*(PPt) *ca.* 2200 Hz] consistent with the presence of the mutually *cis* phosphine centres. The ES mass spectra of **16**, **17** and **18** gave clean peaks at *m*/*z* 1940 [**16** + Na]$^+$, 2698 [**17** + Cs]$^+$ and 2643 [**18** + Na]$^+$ after addition of the appropriate alkali metal ion.

When $NHEt_2$ was used as the base, the adducts *cyclo*-{Pt(μ-C≡CC≡C)(PEt_3)$_2$}$_4$·[NH_2Et_2][OTf] **19**, *cyclo*-{Pt(μ-C≡CC≡C)(dppe)}$_4$·[NH_2Et_2][OTf] **20** and *cyclo*-{Pt(μ-C≡CC≡C)(dppp)}$_4$·[NH_2Et_2][OTf] **21** were obtained, the compositions being assigned on the basis of elemental microanalyses and their IR, NMR and mass spectra. The IR spectra of **19**, **20** and **21** vary little from those of the analogous compounds **16**, **17** and **18**, but contained in addition the characteristic *ν*(SO) and *ν*(CF) bands from the triflate anion at *ca.* 1030, 1225 and 1290 cm^{-1}. Moreover, in the NMR spectra, peaks corresponding to the presence of [NH_2Et_2]$^+$ cations were seen at δ 0.8–1.44 and δ_C 10.93–11.18 for $NH_2(CH_2C\mathit{H}_3)_2$ and δ_H 2.64–3.07 and δ_C 41.41–41.94 for $NH_2(\mathit{CH}_2CH_3)_2$. The ES mass spectrum of **20** in dmso contained a single ion at *m*/*z* 2640 corresponding to [M − OTf]$^+$. MS/MS experiments on this peak showed the formation of the two daughter ions [M − NH_2Et_2OTf]$^+$ (*m*/*z* 2566) and [M − NH_2Et_2OTf − dppe]$^+$ (*m*/*z* 2242). The spectrum of **21** in CH_2Cl_2–MeOH showed a single peak at *m*/*z* 2696 assigned to [M − OTf]$^+$.

A brief survey of the inclusion of substituted ammonium triflates were undertaken by varying the amine used in the preparation of the adduct of **19**. The resulting products were analysed by ES mass spectrometry. When $NHEt_2$ was used, the base peak corresponded to [M − OTf]$^+$ (*m*/*z* 1990), followed by successive losses of up to three PEt_3 ligands which could be followed by MS/MS experiments. Similar results were seen with $NHCy_2$ and $NHPr^i_2$ with [M − OTf]$^+$ peaks at *m*/*z* 2097 and *m*/*z* 2017 respectively. Even with the bulky base dbu (dbu = 1,8-diazabicyclo[5.4.0]undec-7-ene), the adduct gave [M − OTf]$^+$ as the major peak at *m*/*z* 2068. Interestingly, in all cases peaks were also present corresponding to loss of a Pt(PEt_3)$_2$ group, *i.e.* apparent break-up of the square possibly by reductive elimination to form a triangular macrocycle. With the exception of the peaks due to the inclusion of [NH_2Et_2][OTf], the NMR spectra of the adducts **19**, **20** and **21** vary little from those of the "pure" molecular squares.

We note that secondary amines have been used in the pioneering work of Stoddart and his group, as one component of a "molecular meccano kit", specifically the axle or thread of a [2]pseudorotaxane.[45] Non-covalent interactions between the amine hydrogens and the oxygens of appropriate crown ethers afford the supramolecular array. In the present instance, possible association of the amine hydrogens with the C≡C triple bonds, analogous to that found in the chloroform adducts of {Au(PPh_2Fc)}$_2$(μ-C≡C)[46] or N(C_2H_4O)$_3$SiC≡CC≡CSiMe$_3$,[47] for example, may explain the strong attachments found here. Further work is designed to resolve and study further this problem.

Mixed-ligand molecular squares were also obtained by this route, by using combinations of Pt(C≡CC≡CH)(L_2) and Pt(OTf)$_2$(L'_2) where L ≠ L′. In this way, the complexes *cyclo*-Pt_4(μ-C≡CC≡C)$_4$(PEt_3)$_4$(dppe)$_2$·[NH_2Et_2][OTf] **22**, *cyclo*-Pt_4(μ-C≡CC≡C)$_4$(PEt_3)$_4$(dppp)$_2$·[NH_2Et_2][OTf] **23** and *cyclo*-Pt_4(μ-C≡CC≡C)$_4$(dppe)$_2$(dppp)$_2$·[NH_2Et_2][OTf] **24** were prepared in good yield and readily identified by NMR and ES mass spectroscopy. Thus, the ^{1}H NMR spectrum of **22** showed signals arising from the presence of the two different phosphine ligands, at δ 0.12 (Me) and 1.01 (CH_2) for PEt_3 and δ 2.36 and 6.33–7.07 for dppe. The ^{31}P NMR spectra contained two triplets at δ 5.08 [*J*(PPt) = 2338 Hz] and 40.76 [*J*(PPt) = 2323 Hz] for the PEt_3 and dppe ligands, respectively. The ES mass spectrum contained a single peak at *m*/*z* 2314 assigned to [M − OTf]$^+$. Similarly, two triplets at δ −7.69 [*J*(PPt) = 2284 Hz] and 6.15 [*J*(PPt) = 2209 Hz] in the ^{31}P NMR spectrum of **23** arise from the dppp and PEt_3 ligands, respectively. The ES mass spectra contained [M − OTf]$^+$ at *m*/*z* 2344. In the case of **24**, the ^{31}P NMR spectrum contains triplet resonances from dppp and dppe at δ −3.45 [*J*(PPt) = 3408 Hz] and 43.36 [*J*(PPt) = 2288 Hz], respectively. The ES mass spectrum contains [M − OTf]$^+$ at *m*/*z* 2665. No ions corresponding to homo-ligand complexes are present in any of these spectra.

We have not been able to obtain single crystals of any of the substituted ammonium triflate adducts, **19**–**24**, suitable for X-ray studies, so we cannot say how the cation and anion are accommodated by the square molecule. However, that the cation is strongly attached to the neutral complex is shown by its persistence towards extensive extraction with a variety of polar solvents, although it can be removed by washing with aqueous sodium acetate solution.

Molecular structure of *cyclo*-{Pt(μ-C≡CC≡C)(dppe)}$_4$ 17

These molecular squares crystallise with some reluctance. However, using a sample of **17** prepared using NaOAc as base, we obtained single crystals from aqueous dmso on two different occasions as different phases, modelled as 10dmso and as 4.5dmso·H_2O solvates. The following description and discussion are conducted in terms of the former, being representative

Table 3 Selected bond parameters for molecular square *cyclo*-{Pt(C≡CC≡C)(dppe)}$_4$ (**17**)

Pt(1)–P(11)	2.279(4)	C(11)–C(12)	1.17(1)
Pt(1)–P(12)	2.295(2)	C(12)–C(13)	1.40(1)
Pt(2)–P(21)	2.282(2)	C(13)–C(14)	1.22(1)
Pt(2)–P(22)	2.285(4)	C(21)–C(22)	1.24(2)
Pt(1)–C(11)	2.027(8)	C(22)–C(23)	1.38(2)
Pt(1)–C(24)	2.00(1)	C(23)–C(24)	1.21(2)
Pt(2)–C(14)	2.019(8)		
Pt(2)–C(21)	2.00(1)		
P(11)–Pt(1)–P(22)	84.9(1)	C(11)–Pt(1)–C(24)	87.9(4)
P(21)–Pt(2)–P(22)	85.2(1)	C(14)–Pt(2)–C(21)	90.6(4)
P(11)–Pt(1)–C(11)	93.2(3)	Pt(1)–C(11)–C(12)	176(1)
P(11)–Pt(1)–C(24)	178.2(3)	C(11)–C(12)–C(13)	179(1)
P(12)–Pt(1)–C(11)	178.0(3)	C(12)–C(13)–C(14)	178(1)
P(12)–Pt(1)–C(24)	93.9(2)	C(13)–C(14)–Pt(2)	177(1)
P(21)–Pt(2)–C(14)	177.4(4)	Pt(1)–C(24)–C(23)	177.3(8)
P(21)–Pt(2)–C(21)	92.0(2)	C(24)–C(23)–C(22)	177(1)
P(22)–Pt(2)–C(14)	92.1(3)	C(23)–C(22)–C(21)	177.5(9)
P(22)–Pt(2)–C(21)	174.5(3)	C(22)–C(21)–Pt(2)	175.9(8)

and less complex, lying with a crystallographic inversion centre at the centre of the square, of which half is crystallographically independent. Details of the lower solvate are of comparable precision and have been deposited. A plot of a molecule of **17** is shown in Fig. 7, with significant structural parameters being collected in Table 3. Comparison with **2** shows that the Pt–C [1.95–2.03(1) Å], C≡C [1.18–1.22(2) Å], C–C [1.39–1.44(2) Å] and Pt–P distances [2.256–2.285(3) Å] are closely similar; the angles at Pt subtended by the two C_4 edges are between 87.2 and 90.6(5)° in **17**, compared with 93.2(5)° in **2**. Along the edges, angles at the four carbons range between 173 and 179(2)°. The separations of the Pt atoms are 7.726–7.798(1) Å (along the edges) and 10.703, 11.265(1) Å (along the diagonals). For the Pt_4 plane of the monoclinic form, χ^2 is 18696, δPt(1–4) being 0.084, −0.084, 0.083 and −0.083(1) Å, and δP(n1,n2) −0.162, 0.805; 0.173, 0.178; 0.360, −0.302 and 0.109, −0.190(4) Å.

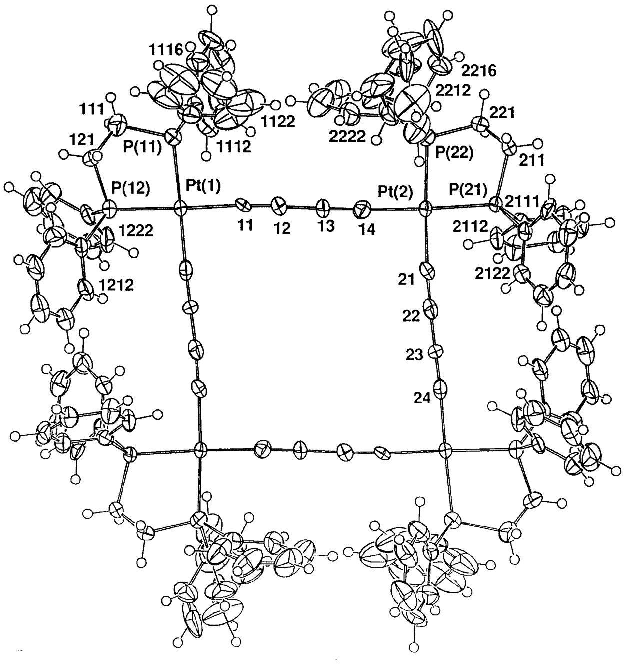

Fig. 7 Molecular projection of *cyclo*-{Pt(μ-C≡CC≡C)(dppe)}$_4$ (**17**), normal to the Pt_4 plane, in the 10dmso solvate, which is centrosymmetric.

As found for **2**, the phenyl groups of the dppe ligands in **17** lie over the C_4 edges and are bent away from the chain and do not interfere sterically with each other. (The angles C(1)–Pt–C(1′) and P–Pt–P′ in **2** are 93.2(5)° and 86.2(1)°, respectively). This is in contrast with the situation for *cyclo*-{Pt(μ-C≡CC≡C)(dppp)}$_4$ **18** in which molecular modelling suggests that significant strain occurs as a result of the proximity of the phenyl rings on adjacent dppp ligands, which are oriented towards each other as a result of the longer $(CH_2)_3$ backbone. In contrast we note that with more bulky edges, the use of dppp has been preferred, because of the tendency for π-stacking to occur between the phenyl groups of the dppp ligand and the aromatic rings of the spacer groups.[1a]

The unit cells of **17** contain additional dmso (and water) molecules. In both phases, the solvent molecules lie about the centre of the square and, more prominently in the deca-solvate, along the edges as well.

Theoretical considerations

In order to understand somewhat the electronic structure of the molecular squares *cyclo*-{Pt(μ-C≡CC≡C)(L)$_2$}$_4$, EH and DF calculations were carried out on the hydrogen-substituted model complex *cyclo*-{Pt(μ-C≡CC≡C)(dHpe)}$_4$ (**17-H**) of D_{4h} symmetry. A rather good agreement is found between the DF optimised and experimental geometries of **17-H** and **17**, respectively. In particular, a slight curvature is computed for the PtC_4Pt sequences of the square as experimentally observed (see Table 3).

The DF MO diagram of the optimised geometry of **17-H** shows a closed-shell electron configuration with a rather large HOMO–LUMO gap of 1.88 eV. A comparable MO diagram is obtained with EH calculations. The same closed-shell electron configuration is obtained, with a comparable HOMO–LUMO gap of 1.82 eV. The composition of the MOs in the HOMO–LUMO region is similar for both DF and EH results. Therefore, because of its structural complexity (large size of the molecule) the detailed analysis of the bonding in **17-H** was carried out using EH calculations.

The qualitative MO diagram of model **17-H** (not shown here) is comparable to that of the monometallic model 2-H shown earlier in Fig. 4. Indeed, as for **2-H**, the LUMOs derive almost exclusively from π* components of the C_4 chains, whereas HOMOs result from strong interactions between d-type metallic FMOs and π components of the carbon units. A set of seven MOs (three in-plane and four out-of-plane), all of which are highly delocalised over the Pt_4C_{16} skeleton and quite close in energy, is found in the HOMO region. All of them are antibonding between Pt and C_α and between C_β and $C_{\beta'}$, but bonding between C_α and C_β.

Owing to the peculiar nature and the energy of the HOMOs computed for **17-H**, the molecular squares *cyclo*-{Pt(μ-C≡CC≡C)L$_2$}$_4$ should be rather easily oxidised without involving important structural changes. Indeed, the first DF ionisation potential computed for model **17-H** is 4.79 eV, which is comparable to that computed for carbon chain-containing molecular wires such as {Ru(PH$_3$)$_2$Cp}$_2$(μ-C≡CC≡C) (4.83 eV) which easily undergo one-electron oxidation processes.[11]

EH Mulliken atomic net charges indicate that, as for **2-H**, the phosphorus atoms are positive (0.64) leading to a substantial amount of negative charge on C_α (−0.46) of the carbon chains. On the other hand, Pt and C_β are nearly neutral (−0.19 and −0.04, respectively).

Incorporation of Group 11 metals into molecular squares

It was of interest to compare the reactivity of the molecular squares towards Group 11 molecules or cations with that described above for the "tweezer" complexes. Internal access to the corners is somewhat more restricted in the square complexes, although not prohibitively so. Indeed, previous examples of Group 11 adducts of platinum-based "tweezer" complexes show that the Group 11 metal is not coplanar with the dialkynyl-platinum unit.[28]

The ES mass spectra of solutions of **20** containing [M^I(NCMe)$_4$]$^+$ (M^I = Cu or Ag) contain new ions corresponding to [M + Cu]$^+$ (*m*/*z* 2629) or [M + Ag + MeCN]$^{2+}$ (*m*/*z* 1356), respectively. Light brown (**25**) or cream (**26**) solids were obtained by addition of $\{Cu(OTf)\}_2C_6H_6$ or AgOTf, respectively, to solutions of **20**, or by adding Pt(OTf)$_2$(dppe) to the adducts obtained from the Group 11 species and **2**. Analytical data are consistent with the formation of 1 : 1 adducts of **17** with M(OTf) (M = Cu or Ag), which also contain one unit of [NH$_2$Et$_2$][OTf], namely [{Pt(C≡CC≡C)(dppe)}$_4$M^I][NH$_2$Et$_2$]-[OTf]$_2$. However, this formulation was not supported by their mass spectra. In their IR spectra two ν(C≡C) absorptions are present (at 2127 and 2088 cm^{-1} for **25**; 2147 and 2088 cm^{-1} for **26**), while their ^{31}P NMR spectra each contain two resonances in ratio 3 : 1, with significantly different chemical shifts and *J*(PPt) values, δ 43.24 [*J*(PPt) = 2246 Hz] and 46.40 [*J*(PPt) = 3598 Hz] for **25** and at δ 42.21 [*J*(PPt) = 2336 Hz] and 44.24 [*J*(PPt) = 3652 Hz] for **26**. As found in the exploratory studies, their ES mass spectra contained ions at *m*/*z* 2629 [**17** + Cu]$^+$ (for **25**) and 1356 [**17** + Ag(MeCN)]$^{2+}$ (for **26**). These data suggest incorporation of a single Cu$^+$ or Ag$^+$ cation into the complex, although we have not yet been able to get structural confirmation of this feature; the larger *J*(PPt) values suggest that some *cis*/*trans* isomerisation may have occurred during the reaction with concomitant reorganisation of the square.

Further examples of these complexes were obtained from reactions between **17** and four equivalents of [M^I(NCMe)$_4$]-[BF$_4$] (M^I = Cu, Ag) in acetonitrile, both yielding cream solids on work-up. The Cu(I) adduct **27** contains two Cu(NCMe)-(BF$_4$) fragments, as shown by ^{1}H, ^{13}C and ^{31}P NMR spectral data. These include two ^{31}P triplets at δ 40.03 [*J*(PPt) = 2275 Hz] and 43.35 [*J*(PPt) = 3604 Hz] in a 1 : 1 ratio. The differences in both the chemical shifts and coupling constants suggested the incorporation of two [Cu(NCMe)]$^+$ cations into two of the corners of the square. The ES mass spectra of **27** contained a doubly-charged ion at *m*/2*z* 1388, corresponding to [M − 2BF$_4$]$^{2+}$. In contrast the silver complex **28** contains four Ag(NCMe)(BF$_4$) units, as determined by NMR and ES mass spectroscopy. The ^{31}P NMR spectrum showed a triplet at δ 42.40 [*J*(PPt) = 2421 Hz] corresponding to the dppe ligand. The ES mass spectrum in MeCN showed peaks at *m*/*z* 3156 corresponding to [M + 4Ag(MeCN)]$^+$, *m*/*z* 3115 for [M + 4Ag + 3MeCN]$^+$ and a doubly charged peak at *m*/2*z* 1540 corresponding to [M + 4Ag + 2MeCN]$^{2+}$. Similar adducts of the molecular square *cyclo*-{Pt(C≡CC≡C)(dcype)}$_4$ containing up to four Ag$^+$ cations have been prepared by addition of AgBF$_4$ or AgOTf to the square and characterised by FAB and MALDI mass spectrometry.[16]

Conclusions

This paper has described the syntheses of several examples of square-planar platinum(II) complexes containing two mutually *cis* buta-1,3-diynyl ligands, which have been used in further condensations with *cis*-Pt(OTf)$_2$(L)$_2$ complexes to give neutral square molecules *cyclo*-{(L)$_2$Pt(μ-C≡CC≡C)$_2$Pt(L′)$_2$}$_2$. Some reactions of the bis(diynyl) complexes with Group 11 cations (in which they act as "molecular tweezers") and other reagents, such as LiBu^t, Co$_2$(μ-dppm)(CO)$_6$ or Ru$_3$(CO)$_{10}$(NCMe)$_2$, in which they show the conventional reactions of substituted 1-alkynes, are reported. Inclusion of Group 11 cations and secondary ammonium cations into the molecular squares has also been found. Accompanying these studies is a limited ES mass spectrometric investigation into the aggregation of diynyl species with various metal cations. Characterisation of several bis(diynyl)platinum complexes and of one example of the molecular squares by X-ray crystallography is described. These results are accompanied by theoretical studies (at the EH and DF levels of theory) of the electronic structures of these two types of complex.

Experimental

General reaction conditions

Reactions were carried out under an atmosphere of nitrogen, but no special precautions were taken to exclude oxygen during work-up. Common solvents were dried and distilled under nitrogen before use. Elemental analyses were performed by the Canadian Microanalytical Service, Delta, B.C., Canada. Preparative TLC was carried out on glass plates (20 × 20 cm) coated with silica gel (Merck 60 GF$_{254}$, 0.5 mm thickness).

Instrumentation

IR: Perkin Elmer 1720X FT IR. NMR: Bruker CXP300 or ACP300 (^{1}H at 300.13 MHz, ^{13}C at 75.47 MHz, ^{31}P at 121.50 MHz) or Varian Gemini 200 (^{1}H at 199.8 MHz, ^{13}C at 50.29 MHz) spectrometers. Spectra were recorded using solutions in 5 mm sample tubes. FAB mass spectra: VG ZAB 2HF (using 3-nitrobenzyl alcohol as matrix, exciting gas Ar, FAB gun voltage 7.5 kV, current 1 mA, accelerating potential 7 kV. ES mass spectra: Finnegan LCQ or VG Platform II. Solutions were directly infused into the instrument.

Reagents

Buta-1,3-diyne,[48] *cis*-PtCl$_2$(PEt$_3$)$_2$,[49] *cis*-Pt(OTf)$_2$(PEt$_3$)$_2$,[3a] *cis*-PtCl$_2$(dppe),[50] *cis*-Pt(OTf)$_2$(dppe),[3a] *cis*-PtCl$_2$(dppp),[51] *cis*-Pt(OTf)$_2$(dppp),[3a] PtCl$_2$(cod),[52] W(C≡CC≡CH)(CO)Cp,[42] Co$_2$(μ-dppm)(CO)$_6$,[53] Ru$_3$(μ-dppm)(CO)$_{10}$,[54] [Cu(NCMe)$_4$]-[BF$_4$],[55] [Ag(NCMe)$_4$][BF$_4$][55] and AuCl(PPh$_3$),[56] were prepared by the cited literature methods.

Buta-1,3-diynyl-platinum complexes

(a) *cis*-Pt(C≡CC≡CH)$_2$(PEt$_3$)$_2$ 1. CuI (10 mg, 0.05 mmol) and buta-1,3-diyne (5.1 mmol as a 2.8 M solution in thf) were added sequentially to a solution of *cis*-PtCl$_2$(PEt$_3$)$_2$ (250 mg, 0.51 mmol) in dmf (12 ml)–NHEt$_2$ (3 ml), and the mixture was stirred for 30 min. Solvents were removed *in vacuo* and the residue was stirred with water (30 ml). The crude material so obtained was washed with several portions of water, methanol and Et$_2$O and then extracted with CH$_2$Cl$_2$. The extracts were concentrated to *ca.* 5 ml and filtered through celite into rapidly stirred hexane. The resulting white precipitate was collected, washed with cold hexane and air dried to give *cis*-Pt(C≡CC≡CH)$_2$(PEt$_3$) **1** (231 mg, 80%). Crystals suitable for the X-ray study were grown from CH$_2$Cl$_2$–hexane by slow diffusion. Anal. Found: C, 43.54; H, 5.73. C$_{20}$H$_{32}$P$_2$Pt·0.5CH$_2$-Cl$_2$ calc.: C, 43.05; H, 5.81%; *M*, 529. IR (Nujol): ν(≡CH) 3249s, ν(C≡C) 2147s cm^{-1}. ^{1}H NMR (CDCl$_3$): δ 1.08 [dt, *J*(HP) = 8 Hz, 18H, Me], 1.81 [t, *J*(HP) = 4.6 Hz, 2H, ≡CH], 1.97 [dq, *J*(HP) = 8 Hz, 12H, CH$_2$]. ^{13}C NMR: δ 8.23 [t, *J*(CP) = 16 Hz, Me], 16.90 (m, CH$_2$), 60.89 (s, C$_\delta$), 72.04 (s, C$_\gamma$), 80.97 (s, C$_\beta$), 94.69 (s, C$_\alpha$). ^{31}P NMR (d_6-dmso): δ 5.44 [s, *J*(PPt) = 2262 Hz, PEt$_3$]. ES mass spectrum (in MeOH containing NaOMe, *m*/*z*): 1081, [2M + Na]$^+$; 552, [M + Na]$^+$.

(b) Pt(C≡CC≡CH)$_2$(dppe) 2. Similarly, PtCl$_2$(dppe) (1.0 g, 1.5 mmol) in dmf–NHEt$_2$ (45 : 15 ml), CuI (30 mg, 0.15 mmol) and buta-1,3-diyne (15 mmol as a 2.8 M solution in thf) were stirred for 15 min. Work-up gave a white precipitate of Pt(C≡CC≡CH)$_2$(dppe) **2** (1.0 g, 96%). Crystals suitable for X-ray study were grown from CH$_2$Cl$_2$–hexane by slow diffusion. Anal. Found: C, 59.25; H, 3.76. C$_{34}$H$_{26}$P$_2$Pt calc.: C, 59.09; H, 3.76%; *M*, 691. IR (Nujol): ν(≡CH) 3288w, ν(C≡C) 2147s cm^{-1}. ^{1}H NMR (CDCl$_3$): δ 1.82 [t, *J*(HP) = 4Hz, 1H, ≡CH], 2.42 [m, 2H, P(CH$_2$)$_2$P], 7.44–7.89 (m, 10H, PPh$_2$). ^{13}C NMR (CDCl$_3$): δ 27.80 (unresolved dd, CH$_2$P), 61.74 (s, C$_\gamma$), 71.75 (s, C$_\delta$), 77.21 (s, C$_\beta$), 93.70 (s, C$_\alpha$), 128.41–133.53 (m, Ph). ^{31}P NMR (d_6-dmso): δ 43.26 [s, *J*(PPt) = 2288 Hz]. FAB mass spectrum (*m*/*z*): 692, [M + H]$^+$; 642, [M + H − C$_4$H]$^+$; 593, [M − 2C$_4$H]$^+$. ES mass spectrum (MeCN + Ag$^+$, *m*/*z*): 1491, [2M + Ag]$^+$; 839, [M + Ag + MeCN]$^+$; 799, [M + Ag]$^+$.

(c) $Pt(C\equiv CC\equiv CH)_2(dppp)$ 3. A mixture of $PtCl_2(dppp)$ (1.0 g, 1.47 mmol) in dmf–$NHEt_2$ (45 : 15 ml), CuI (30 mg, 0.15 mmol) and buta-1,3-diyne (15 mmol as a 2.8 M solution in thf) was stirred for 30 min. Concentration and addition of water gave white $Pt(C\equiv CC\equiv CH)_2(dppp)$ **3** (831 mg, 80%). Crystals suitable for the X-ray study were grown from CH_2Cl_2–hexane by slow diffusion. Anal. Found: C, 59.51; H, 4.08. $C_{34}H_{28}P_2Pt$ calc.: C, 59.57; H, 4.00%; *M*, 705. IR (Nujol): $\nu(\equiv CH)$ 3296s, $\nu(C\equiv C)$ 2151s cm^{-1}. ^1H NMR (d_6-dmso): δ 1.71 [t, *J*(HP) = 23Hz, 2H, ≡CH], 2.70 [m, 6H, $P(CH_2)_3P$], 7.31–7.72 (m, 20H, PPh_2). ^{13}C NMR (d_6-dmso): δ 64.40 (s, C_δ), 72.02 (s, C_γ), 128.23–133.41 (m, Ph). ^{31}P NMR (d_6-dmso): δ −6.69 [s, *J*(PPt) = 2204 Hz, dppp]. ES mass spectrum (MeOH + Ag$^+$, *m*/*z*): 1519, [2M + Ag]$^+$; 813, [M + Ag]$^+$.

(d) $Pt(C\equiv CC\equiv CH)_2(cod)$ 4. To a solution of $PtCl_2(cod)$ (200 mg, 0.54 mmol) in dmf–$NHEt_2$ (5 : 3 ml), CuI (9 mg, 0.05 mmol) was added followed by buta-1,3-diyne (5.4 mmol as a 2.2 M solution in thf). The solution was stirred at room temperature for 15 min and the solvent was removed. Water (10 ml) was then added and $Pt(C\equiv CC\equiv CH)_2(cod)$ **4** separated as a brown sticky solid, which rapidly decomposes upon attempted isolation (121 mg, 56%). IR (Nujol): $\nu(C\equiv CH)$ 3270, $\nu(C\equiv C)$ 2131 cm^{-1}. The complex is very unstable in solution. However, addition of dppe (213 mg, 0.54 mmol) in EtOH (15 ml) and stirring at rt for 15 min gave $Pt(C\equiv CC\equiv CH)_2(dppe)$ **2** (368 mg, 99%) after precipitation from cold hexane.

Reactions of $Pt(C\equiv CC\equiv CH)_2(dppe)$ 2

(a) $Pt\{C\equiv CC_2H[Co_2(\mu\text{-}dppm)(CO)_4]\}_2(dppe)$ 5. A mixture of **2** (100 mg, 0.15 mmol) and $Co_2(\mu\text{-}dppm)(CO)_6$ (193 mg, 0.29 mmol) in thf (20 ml) was heated under reflux for 30 min. TLC showed the formation of a burgundy coloured compound. Solvent was removed and the residue was dissolved in CH_2Cl_2 and chromatographed on silica plates (acetone : hexane, 2 : 3). A burgundy band (R_f = 0.65) was collected and recrystallised from CH_2Cl_2–pentane to give dark red crystals of $Pt\{C\equiv CC_2H[Co_2(\mu\text{-}dppm)(CO)_4]\}_2(dppe)$ **5** (140 mg, 50%). Anal. Found: C, 57.30; H, 3.63. $C_{92}H_{70}Co_2O_8P_6Pt$ calc.: C, 57.54; H, 3.67%; *M*, 1919. IR (CH_2Cl_2): $\nu(CO)$ 2016, 1990, 1960 cm^{-1}. ^1H NMR ($CDCl_3$): δ 1.86 (s, 2H, C_2H), 2.45 (m, 4H, dppe-CH_2), 3.53 (m, 4H, 2 × dppm CH_2), 6.98–7.99 (m, 60H, Ph). ^{13}C NMR ($CDCl_3$): δ 29.05 (m, CH_2), 29.57 (m, CH_2), 127.65–138.46 (m, Ph). ^{31}P NMR ($CDCl_3$): δ 20.66 (s, dppm), 34.96 [s, *J*(PtP) = 2259 Hz, dppe]. ES mass spectrum (CH_2Cl_2, *m*/*z*): 1920, M$^-$; 1892–1696, [M − *n*CO]$^-$ (*n* = 1–8).

(b) $Ru_3(\mu\text{-}H)\{\mu_3\text{-}\eta^2\text{-}C_2C\equiv C[Pt(C\equiv CC\equiv CH)(dppe)]\}(\mu\text{-}dppm)(CO)_7$ 6. A mixture of $Ru_3(CO)_{10}(dppm)$ (100 mg, 0.1 mmol) and **2** (69 mg, 0.1 mmol) in thf (30 ml) was heated at reflux point for 10 h. Solvent was removed and the residue extracted with CH_2Cl_2 and purified by TLC (silica gel, acetone : hexane, 4 : 6). The yellow band (R_f 0.5) was collected and recrystallised from CH_2Cl_2–hexane to give $Ru_3(\mu\text{-}H)\{\mu_3\text{-}\eta^2\text{-}C_2C\equiv C[Pt(C\equiv CC\equiv CH)(dppe)]\}(\mu\text{-}dppm)(CO)_7$ **6** (88.3 mg, 56%). Anal. Found: C, 50.02; H, 3.07. $C_{69}H_{48}O_{10}P_4PtRu_3$ calc.: C, 49.95; H, 2.92%; *M*, 1577. IR (CH_2Cl_2): $\nu(CO)$ 2060m, 2054s, 1999m, 1943(br) cm^{-1}. ^1H NMR ($CDCl_3$): δ −19.39 [d, *J*(PtH) = 34 Hz, 1H, RuH], 2.36 (m, 4H, dppe), 3.45 (m, 2H, dppm), 4.36 (m, 2H, dppm), 6.65–8.05 (m, 40H, Ph). ^{13}C NMR ($CDCl_3$): δ 28.89 (s, CH_2), 29.70 (s, CH_2), 128.48–133.88 (m, Ph). ES mass spectrum (CH_2Cl_2 containing NaOMe, *m*/*z*): 1607, [M + OMe]$^-$; 1575, [M − H]$^-$; 1547–1463, [M − *n*CO]$^-$ (*n* = 1–4).

(c) $Pt(C\equiv CC\equiv CMe)_2(dppe)$ 7. A solution of **2** (100 mg, 0.15 mmol) in thf (15 ml) was cooled to −30 °C. $LiBu^t$ (260 µl, 0.43 mmol) was added *via* syringe and the yellow solution was stirred for 10 min, when the colour had darkened to orange. MeI (82 mg, 0.58 mmol) was added and the resulting solution warmed to room temperature. MeOH was added to give a cream precipitate, which was collected and washed with EtOH, MeOH, Et_2O and hexane and then air-dried to give $Pt(C\equiv CC\equiv CMe)_2(dppe)$ **7** (97 mg, 93%). IR (Nujol): $\nu(C\equiv C)$ 2148s, 2082m cm^{-1}. ^1H NMR ($CDCl_3$): δ 1.28 (br s, 6H, CH_3), 2.39 (m, 4H, CH_2), 7.40–7.83 (m, 20H, Ph). ^{13}C NMR ($CDCl_3$): δ 28.25 (m, dppe-CH_2), 50.76 (s, Me), 61.71 (s, C_δ), 71.81 (s, C_γ), 93.09 (s, C_β), 96.96 (s, C_α), 128.48–133.95 (m, dppe-Ph). ES mass spectrum (CH_2Cl_2–MeOH, *m*/*z*): 726, [M + Li]$^+$; 719, M$^+$.

(d) $Pt(C\equiv CC\equiv CH)(C\equiv CC\equiv CSiMe_3)(dppe)$ 8. Similarly, $LiBu^t$ (260 µl of a 1.7 M pentane solution, 0.43 mmol) was added to **2** (100 mg, 0.15 mmol) in thf (15 ml) at −30 °C. $SiClMe_3$ (630 µl, 0.58 mmol) was then added and the resulting solution was warmed to room temperature. MeOH was added to give a cream precipitate, which was collected and washed with EtOH, MeOH, Et_2O and hexane. A CH_2Cl_2 extract of the solid was added dropwise to cold hexane to give $Pt(C\equiv CC\equiv CH)(C\equiv CC\equiv CSiMe_3)(dppe)$ **8** (75 mg, 68%). Anal. Found: C, 58.43; H, 4.56. $C_{37}H_{34}P_2PtSi$ calc.: C, 58.10; H, 4.40%; *M*, 763. IR (Nujol): $\nu(C\equiv C)$ 2149s, 2089m cm^{-1}. ^1H NMR ($CDCl_3$): δ 0.07 (s, 9H, $SiMe_3$), 1.75 (s, 1H, ≡CH), 2.34 (m, 4H, CH_2), 7.41–7.79 (m, 20H, Ph). ^{13}C NMR ($CDCl_3$): δ 1.30 (s, $SiMe_3$), 28.83 (m, dppe-CH_2), 79.07 (m, C≡C), 126.8–133.63 (m, dppe-Ph).

(e) $Pt(C\equiv CC\equiv CH)\{C\equiv CC\equiv C[Au(PPh_3)]\}(dppe)$ 9. *Method (i).* As above, $LiBu^t$ (260 µl of a 1.7 M pentane solution, 0.43 mmol) was then added to **2** (100 mg, 0.15 mmol) dissolved in thf (15 ml) and cooled to −30 °C. $AuCl(PPh_3)$ (142 mg, 0.29 mmol) was then added and the resulting solution allowed to warm to room temperature. MeOH was added to give a cream precipitate, which was collected and washed with EtOH, MeOH, Et_2O and hexane and then air-dried to give $Pt(C\equiv CC\equiv CH)\{C\equiv CC\equiv C[Au(PPh_3)]\}(dppe).CH_2Cl_2$ **9** (198 mg, 60%). Anal. Found: C, 50.63; H, 3.43. $C_{52}H_{40}AuP_3Pt$ calc.: C, 51.55; H, 3.42%; *M*, 1149. IR (Nujol): $\nu(C\equiv C)$ 2140m, 2084m cm^{-1}. ^1H NMR (dmso): δ 1.22 (s, 1H, ≡CH), 2.32 (m, 4H, CH_2), 7.28–7.83 (m, 35H, Ph). ^{13}C NMR (dmso): δ 27.11 (m, CH_2), 128.85–133.85 (m, Ph). ES mass spectrum (CH_2Cl_2–MeOH, *m*/*z*): 1150, [M + H]$^+$.

Method (ii). Alternatively, addition of a catalytic amount of CuI (≈3 mg, 0.015 mmol) followed by $AuCl(PPh_3)$ (143 mg, 0.29 mmol) to **2** (100 mg, 0.145 mmol in $NHEt_2$–thf (5 ml : 10 ml) and stirring at room temperature for 1 h resulted in the formation of a cream precipitate of $Pt(C\equiv CC\equiv CH)\{C\equiv CC\equiv C[Au(PPh_3)]\}(dppe)$ **9** (115mg, 69%).

Reactions of $Pt(C\equiv CC\equiv CH)_2(dppe)$ 2 with Group 11 substrates

(a) $Cu(SCN)\{(HC\equiv CC_2)_2Pt(dppe)\}$ 10. A mixture of **2** (100 mg, 0.15 mmol) and Cu(SCN) (36 mg, 0.29 mmol) in MeCN (20 ml) was kept at room temperature for 1 h, the yellow solution changing to cream–orange. After filtering and evaporation of solvent, extraction of the residue with CH_2Cl_2 followed by dropwise addition to cold hexane gave an orange precipitate of $Cu(SCN)\{(HC\equiv CC_2)_2Pt(dppe)\}$ **10** (112 mg, 95%). IR (CH_2Cl_2): $\nu(C\equiv C)$ 2098m, $\nu(CN)$ 2155s cm^{-1}. ^1H NMR ($CDCl_3$): δ 1.77 (unresolved m, 1H, ≡CH), 2.35 (m, 4H, dppe-CH_2), 7.16–7.83 (m, 20H, dppe-Ph). ^{13}C NMR ($CDCl_3$): δ 28.09 (m, dppe-CH_2), 61.72 (s, C_δ), 71.80 (s, C_γ), 93.11 (s, C_β), 100.00 (s, C_α), 128.47–133.47 (m, dppe-Ph). ^{31}P NMR ($CDCl_3$): δ 37.13 [s, *J*(PPt) = 2297 Hz, dppe]. ES mass spectrum (CH_2Cl_2–MeOH, *m*/*z*): 1446, [2(**2**) + Cu]$^+$; 755, [**2** + Cu]$^+$; 691, [**2**]$^+$.

(b) $Ag(SCN)\{(HC\equiv CC_2)_2Pt(dppe)\}$ 11. Similarly, **2** (100 mg, 0.15 mmol) and Ag(SCN) (48 mg, 0.29 mmol) in MeCN (20 ml) were stirred at rt for 1 h, the yellow solution changing to cream–yellow. The filtered solution was evaporated and a CH_2Cl_2

extract of the residue added dropwise to cold hexane to give a cream precipitate of Ag(SCN){(HC≡CC$_2$)$_2$Pt(dppe)} **11** (124 mg, 99%). IR (CH$_2$Cl$_2$): *ν*(C≡C) 2093m, *ν*(CN) 2154s cm^{-1}. ^{1}H NMR (CDCl$_3$): *δ* 1.77 [t, 1H, *J*(PH) = 4.2 Hz, ≡CH], 2.32 (m, 4H, dppe-CH$_2$), 7.41–7.83 (m, 20H, dppe-Ph). ^{13}C NMR (CDCl$_3$): *δ* 27.72 (s, dppe-CH$_2$), 61.75 (s, C$_\delta$), 71.77 (s, C$_\beta$), 93.60 (s, C$_\alpha$), 107.92 (s, C$_\alpha$), 128.45–133.53 (m, dppe-Ph). ^{31}P NMR (CDCl$_3$): *δ* 41.16 [s, *J*(PPt) = 2302.93 Hz, dppe]. ES mass spectrum (dmso, *m*/*z*): 1490, [2(**2**) + Ag]$^+$; 798, [**2** + Ag]$^+$. MS^2 on *m*/*z* 1490 gave daughter ions at *m*/*z* 1441 [2(**2**) + Cu − NC$_4$H]$^+$, *m*/*z* 1381 [2(**2**)]$^+$ and *m*/*z* 798 [**2** + Ag]$^+$.

(c) [Cu(NCMe){(HC≡CC$_2$)$_2$Pt(dppe)}]BF$_4$] 12. Similarly, **2** (150 mg, 0.22 mmol) and [Cu(NCMe)$_4$][BF$_4$] (41 mg, 0.217 mmol) in MeCN (20 ml) gave cream [Cu(NCMe){(HC≡CC$_2$)$_2$-Pt(dppe)}][BF$_4$] **12** (154 mg, 80%). Anal. Found: C, 48.88; H, 3.38. C$_{36}$H$_{29}$BF$_4$NP$_2$CuPt calc.: C, 48.97; H, 3.31%; *M*, 883. IR (Nujol): *ν*(C≡CH) 3281m; *ν*(C≡C) 2139m; *ν*(BF) 1060s cm^{-1}. ^{1}H NMR (CDCl$_3$): *δ* 1.75 (s, 2H, ≡CH), 2.00 (s, 3H, MeCN), 2.53 (m, 4H, dppe-CH$_2$), 7.46–7.72 (m, 20H, dppe-Ph). ^{13}C NMR (CDCl$_3$): *δ* 1.82 (s, *Me*CN), 29.67 (s, dppe-CH$_2$), 65.33 (s, C$_\delta$), 67.56 (C$_\gamma$), 77.42 (C$_\beta$), 99.21 (s, C$_\alpha$), 116.29 (s, CH$_3$*C*N), 129.29–133.02 (m, dppe-Ph). ^{31}P NMR (CD$_3$CN): *δ* 42.18 [s, *J*(PPt) = 2409 Hz, dppe]. ES mass spectrum (MeCN, *m*/*z*): 1446, [2(**2**) + Cu]$^+$; 1396, [2(**2**) + Cu − C$_4$H]$^+$; 796, [**2** + Cu + NCMe]$^+$; 755, [**2** + Cu]$^+$.

(d) [Ag(NCMe){(HC≡CC$_2$)$_2$Pt(dppe)}][BF$_4$] 13. A solution of **2** (150 mg, 0.22 mmol) and [Ag(NCMe)$_4$][BF$_4$] (51 mg, 0.22 mmol) in MeCN (20 ml) was stirred at rt for 1 h. After evaporation, a CH$_2$Cl$_2$ extract (5 ml) was added dropwise to cold rapidly stirred Et$_2$O (100 ml) to give a cream precipitate of [Ag(NCMe){(HC≡CC$_2$)$_2$Pt(dppe)}][BF$_4$] **13** (124 mg, 62%). Anal. Found: C, 46.88; H, 3.28. C$_{36}$H$_{29}$BF$_4$NP$_2$AgPt calc.: C, 46.58; H, 3.15%; *M*, 928. IR (Nujol): *ν*(≡CH) 3255m, *ν*(C≡C) 2141m, *ν*(BF) 1061s cm^{-1}. ^{1}H NMR (CD$_3$CN): *δ* 1.95 (s, 2H, ≡CH), 2.00 (s, 3H, MeCN), 2.41 (m, 4H, dppe-CH$_2$), 7.36–7.65 (m, 20H, dppe-Ph). ^{13}C NMR (CD$_3$CN): *δ* 1.18 (s, MeCN), 28.33 (m, dppe-CH$_2$), 65.96 (s, C$_\delta$), 69.60 (s, C$_\delta$), 79.29 (s, C$_\beta$), 102.54 (s, C$_\alpha$), 129.92–134.27 (m, dppe-Ph). ^{31}P NMR (CD$_3$CN): *δ* 46.23 [s, *J*(PPt) = 2434 Hz]. ES mass spectrum (MeCN, *m*/*z*): 1491, [2(**2**) + Ag]$^+$; 1441, [2(**2**) + Ag − C$_4$H]$^+$; 839, [**2** + Ag + MeCN]$^+$; 799, [**2** + Ag]$^+$.

Construction of molecular squares

(a) *cyclo*-{Pt(μ-C≡CC≡C)(PEt$_3$)$_2$}$_4$ 16. A solution of NaOAc (76 mg, 538 mmol) in MeOH (10 ml) was added to **1** (72.5 mg, 0.14 mmol) in CH$_2$Cl$_2$ (50 ml). Pt(OTf)$_2$(PEt$_3$)$_2$ (100 mg, 0.14 mmol) in CH$_2$Cl$_2$ (10 ml) was added to this mixture *via* syringe pump over a period of 2 h during which time the initial pale yellow solution darkened in colour. Removal of solvent, extraction with CH$_2$Cl$_2$ (5 ml) and filtration into rapidly stirred cold hexane gave a cream precipitate of *cyclo*-{Pt(μ-C≡CC≡C)-(PEt$_3$)$_2$}$_4$ **16** (183 mg, 70%). Anal. Found: C, 40.43; H, 5.97. C$_{64}$H$_{120}$P$_8$Pt$_4$ calc.: C, 40.07; H, 6.31%; *M*, 1917. IR (Nujol): *ν*(C≡C) 2144 cm^{-1}. ^{1}H NMR (*d*$_6$-dmso): *δ* 1.02 (m, 72H, PCH$_2$*CH*$_3$), 1.92 (m, 48H, P*CH*$_2$CH$_3$). ^{13}C NMR (*d*$_6$-dmso): *δ* 8.07 (s, PCH$_2$*CH*$_3$), 16.48 [dq, *J*(CP) = 17.13 Hz, P*CH*$_2$CH$_3$]. ^{31}P NMR (*d*$_6$-dmso): *δ* −0.40 [s, *J*(PPt) = 2260 Hz, PEt$_3$]. ES mass spectrum (CH$_2$Cl$_2$–MeOH with NaOMe, *m*/*z*): 1940, [M + Na]$^+$.

(b) *cyclo*-{Pt(μ-C≡CC≡C)(dppe)}$_4$ 17. Similarly, addition of Pt(OTf)$_2$(dppe) (100 mg, 0.11 mmol) in CH$_2$Cl$_2$ (10 ml) to a mixture of **2** (77.5 mg, 0.11 mmol) in CH$_2$Cl$_2$ (50 ml) and NaOAc (61 mg, 0.45 mmol) in MeOH (5 ml) gave a cream precipitate of *cyclo*-{Pt(μ-C≡CC≡C)(dppe)}$_4$ **17** (207 mg, 72%). Anal. Found: C, 55.86; H, 3.77. C$_{120}$H$_{96}$P$_8$Pt$_4$ calc.: C, 56.17; H, 3.77%; *M*, 2566. IR (Nujol): *ν*(C≡C) 2148m cm^{-1}. ^{1}H NMR (*d*$_6$-dmso): *δ* 2.35 (m, 4H, CH$_2$), 7.08–7.73 (m, 20H, Ph). ^{13}C NMR (*d*$_6$-dmso): *δ* 24.10 (m, CH$_2$ dppe), 128.69–133.25 (m, Ph dppe). ^{31}P NMR (*d*$_6$-dmso): *δ* 43.32 [s, *J*(PPt) = 3605 Hz, dppe]. ES mass spectrum (CH$_2$Cl$_2$–MeOH + Cs$^+$, *m*/*z*): 2698, [M + Cs]$^+$.

(c) *cyclo*-{Pt(μ-C≡CC≡C)(dppp)}$_4$ 18. Similarly, **3** (78 mg, 0.11 mmol) in CH$_2$Cl$_2$ (50 ml) with NaOAc (60 mg, 0.44 mmol) in MeOH (10 ml) was treated with Pt(OTf)$_2$(dppp) (100 mg, 0.11 mmol) in CH$_2$Cl$_2$ (10 ml). Removal of solvent followed by addition of hexane resulted in the precipitation of cream *cyclo*-{Pt(μ-C≡CC≡C)(dppp)}$_4$ **18** (210 mg, 73%). Anal. Found: C, 56.29; H, 3.89. C$_{124}$H$_{104}$P$_8$Pt$_4$ calc.: C, 56.78; H, 4.00%; *M*, 2621. IR (Nujol): *ν*(C≡C) 2148m cm^{-1}. ^{1}H NMR (*d*$_6$-dmso): *δ* 2.60 (m, 6H, dppp CH$_2$), 7.05–7.74 (m, 20H, dppp Ph). ^{13}C NMR (*d*$_6$-dmso): *δ* 24.78 (m, dppp CH$_2$), 127.56–133.74 (m, dppp Ph). ^{31}P NMR (*d*$_6$-dmso): *δ* −7.69 [s, *J*(PPt) = 2188 Hz, dppp]. ES mass spectrum (CH$_2$Cl$_2$–MeOH + NaOMe, *m*/*z*): 2644, [M + Na]$^+$.

(d) *cyclo*-{Pt(μ-C≡CC≡C)(PEt$_3$)$_2$}$_4$·[NH$_2$Et$_2$][OTf] 19. *cis*-Pt(OTf)$_2$(PEt$_3$)$_2$ (68 mg, 0.09 mmol) in CH$_2$Cl$_2$ (10 ml) was slowly added *via* syringe pump over 2 h to **1** (50 mg, 0.09 mmol) in CH$_2$Cl$_2$ (50 ml) containing NHEt$_2$ (1 ml). The initial pale yellow solution darkened to a light orange–brown. Partial evaporation and filtration into stirred hexane gave a cream precipitate of *cyclo*-{Pt(μ-C≡CC≡C)(PEt$_3$)$_2$}$_4$·[NH$_2$Et$_2$][OTf] **19** (121 mg, 63%). Anal. Found: C, 38.27; H, 6.47. C$_{69}$H$_{132}$-F$_3$NO$_3$P$_8$Pt$_4$S calc.: C, 38.71; H, 6.21%; *M*, 2138. IR (Nujol): *ν*(C≡C) 2136m, *ν*(OTf) 1254m, 1222m, 1030m cm^{-1}. ^{1}H NMR (*d*$_6$-dmso): *δ* 0.64 [dt, *J*(HP) = 7.5 Hz, 72H, PCH$_2$*Me*], 0.83 [dd, *J*(HH) = 6.3 Hz, 48H, NH$_2$(CH$_2$*Me*)$_2$], 1.56 [t, *J*(HH) = 6.9 Hz, 6H, P*CH*$_2$Me], 2.64 (unresolved m, 4H, NH$_2$(*CH*$_2$Me)$_2$). ^{13}C NMR (*d*$_6$-dmso): *δ* 8.21 (s, PCH$_2$*Me*), 11.04 (s, NH$_2$(CH$_2$*Me*)$_2$), 16.65 [dq, *J*(CP) = 17.13 Hz, P*CH*$_2$Me], 41.60 (s, NH$_2$-(*CH*$_2$Me)$_2$), 93.09 (m, C$_\beta$) 94.98 (m, C$_\alpha$). ^{31}P NMR (*d*$_6$-dmso): *δ* −0.43 [s, *J*(PPt) = 2260 Hz, PEt$_3$]. ES mass spectrum (MeOH, *m*/*z*; M ≡ **19**): 1990, [M + NH$_2$Et$_2$]$^+$; 1635, [M + NH$_2$Et$_2$ − 3PEt$_3$]$^+$; 1559, [M + NH$_2$Et$_2$ − Pt(PEt$_3$)$_2$]$^+$. MS^2 on *m*/*z* 1990 gave one daughter ion at *m*/*z* 1559 [M + NH$_2$Et$_2$- Pt(PEt$_3$)$_2$]$^+$. MS^3 on *m*/*z* 1559 gave two daughter ions at *m*/*z* 1485 [M − NH$_2$Et$_2$]$^+$ and *m*/*z* 1368 [M − Pt(PEt$_3$)$_2$ − PEt$_3$]$^+$. MS^4 on *m*/*z* 1485 gave one daughter ion at *m*/*z* 1368 [M − Pt(PEt$_3$)$_2$ −2PEt$_3$]$^+$. MS^5 on *m*/*z* 1368 gave one daughter ion at *m*/*z* 1251 [M − Pt(PEt$_3$)$_2$ − 3PEt$_3$]$^+$.

Similar preparations were carried out using NHCy$_2$, NHPr$^i_2$ and dbu as bases for the reaction between **1** and *cis*-Pt(OTf)$_2$-(PEt$_3$)$_2$. The following products were characterised by ES mass spectroscopy (M ≡ **19**):

(i) NHCy$_2$: ES mass spectrum (CH$_2$Cl$_2$, *m*/*z*): 2099, [M + NH$_2$Cy$_2$]$^+$; 1668, [M + NH$_2$Cy$_2$ − Pt(PEt$_3$)$_2$]$^+$. MS^2 on *m*/*z* 2099 gave one daughter ion at *m*/*z* 1668 [M + NH$_2$Cy$_2$- Pt(PEt$_3$)$_2$]$^+$.

(ii) NHPr$^i_2$: ES mass spectrum (CH$_2$Cl$_2$, *m*/*z*): 2019, [M + NH$_2$Pr$^i_2$]$^+$; 1587, [M + NH$_2$Pr$^i_2$ − Pt(PEt$_3$)$_2$]$^+$. MS^2 on *m*/*z* 2019 gave two daughter ions at *m*/*z* 1585 [M + NH$_2$Pr$^i_2$- Pt(PEt$_3$)$_2$]$^+$ and *m*/*z* 1487 [M − Pt(PEt$_3$)$_2$]$^+$.

(iii) dbu: ES mass spectrum (CH$_2$Cl$_2$, *m*/*z*): 2068, [M + dbuH]$^+$; 1639, [M + dbuH − Pt(PEt$_3$)$_2$]$^+$.

(e) *cyclo*-{Pt(μ-C≡CC≡C)(dppe)}$_4$·[NH$_2$Et$_2$][OTf] 20. As for **19**, a cream precipitate of *cyclo*-{Pt(μ-C≡CC≡C)(dppe)}$_4$·[NH$_2$Et$_2$][OTf] **20** (181 mg, 58%) was obtained from **2** (77.5 mg, 0.11 mmol) in CH$_2$Cl$_2$ (50 ml) containing NHEt$_2$ (1 ml) and Pt(OTf)$_2$(dppe) (100 mg, 0.11 mmol) in CH$_2$Cl$_2$ (10 ml). Anal. Found: C, 53.82; H, 3.75; N, 0.49. C$_{125}$H$_{108}$F$_3$NO$_3$P$_8$Pt$_4$S calc.: C, 53.82; H, 3.90; N, 0.50%; *M*, 2788. IR (Nujol): *ν*(C≡C) 2148m, *ν*(OTf) 1274m, 1223m, 1032m cm^{-1}. ^{1}H NMR (*d*$_6$-dmso): *δ* 1.34 [t, *J*(HH) = 9.6 Hz, 6H, NH$_2$(CH$_2$*Me*)$_2$], 2.32 (m, 4H, CH$_2$), 3.05 [q, *J*(HH) = 6.6 Hz, 4H, NH$_2$(*CH*$_2$Me)$_2$], 7.11–7.83 (m, 20H, Ph). ^{13}C NMR (*d*$_6$-dmso): *δ* 10.93 [s, NH$_2$(CH$_2$*Me*)$_2$], 27.48 (m, CH$_2$ dppe), 41.41 [s, NH$_2$(*CH*$_2$Me)$_2$], 92.23 (m, C$_\alpha$), 110.39 (m, C$_\beta$), 127.03–133.26 (m, Ph). ^{31}P NMR

(d_6-dmso): δ 39.63 [s, *J*(PPt) = 2257 Hz, dppe]. ES mass spectrum (dmso, *m*/*z*; M ≡ **17**): 2639, $[M + NH_2Et_2]^+$. MS^2 on *m*/*z* 2639 gave two daughter ions at *m*/*z* 2565 $[M]^+$ and *m*/*z* 2241 $[M + NH_2Et_2 - dppe]^+$.

(f) *cyclo*-{Pt(μ-C≡CC≡C)(dppp)}$_4$·[NH$_2$Et$_2$][OTf] 21. Similarly, the reaction between **3** (78 mg, 0.11 mmol) and Pt(OTf)$_2$(dppp) (100 mg, 0.11 mmol) gave cream *cyclo*-{Pt(μ-C≡CC≡C)(dppp)}$_4$·[NH$_2$Et$_2$][OTf] **21** (195 mg, 68%). Anal. Found: C, 54.92; H, 4.30; N, 0.50. $C_{129}H_{116}F_3NO_3P_8Pt_4S$ calc.: C, 54.45; H, 4.11; N, 0.49%; *M*, 2845. IR (Nujol): *ν*(C≡C) 2148m, *ν*(OTf) 1274m, 1223m, 1032m cm^{-1}. ^{1}H NMR (d_6-dmso): δ 1.44 [t, *J*(HH) = 6.9 Hz, 6H, NH$_2$(CH$_2$*Me*)$_2$], 2.44 (m, 6H, CH$_2$), 3.07 [q, *J*(HH) = 7.2 Hz, 4H, NH$_2$(*CH$_2$*Me)$_2$], 6.89–7.52 (m, 20H, Ph). ^{13}C NMR (d_6-dmso): δ 11.18 [s, NH$_2$(CH$_2$*Me*)$_2$], 18.72 (m, CH$_2$), 24.51 (m, CH$_2$), 41.94 [s, NH$_2$(*CH$_2$*Me)$_2$], 109.23 (s, C≡C), 127.70–137.66 (m, dppp Ph). ^{31}P NMR (d_6-dmso): δ −8.02 [s, *J*(PPt) = 2189 Hz, dppp]. ES mass spectrum (CH$_2$Cl$_2$/MeOH, *m*/*z*): 2695, [**21** − OTf]$^+$.

(g) *cyclo*-{Pt$_4$(μ-C≡CC≡C)$_4$(PEt$_3$)$_4$(dppe)$_2$}·[NH$_2$Et$_2$][OTf] 22. Similarly, **2** (100 mg, 0.15 mmol) and Pt(OTf)$_2$(PEt$_3$)$_2$ (105 mg, 0.15 mmol) gave cream *cyclo*-{Pt$_4$(μ-C≡CC≡C)$_4$(PEt$_3$)$_4$(dppe)$_2$}·[NH$_2$Et$_2$][OTf] **22** (203 mg, 56%). Anal. Found: C, 47.43; H, 4.46; N, 0.60. $C_{97}H_{120}F_3NO_3P_8Pt_4S$ calc.: C, 47.26; H, 4.90; N, 0.57%; *M*, 2464. IR (Nujol): *ν*(C≡C) 2131m, *ν*(OTf) 1272m, 1223m, 1032m cm^{-1}. ^{1}H NMR (d_6-dmso): δ 0.12 [m, 36H, P(CH$_2$*Me*)$_3$], 1.01 [m, 24H, P(*CH$_2$*Me)$_3$], 1.70 [m, 6H, NH$_2$(CH$_2$*Me*)$_2$], 2.36 (m, 8H, dppe CH$_2$), 6.33–7.07 (m, 40H, dppe Ph). ^{13}C NMR (d_6-dmso): δ 2.67 [s, P(CH$_2$*Me*)$_3$], 7.38 [s, P(*CH$_2$*Me)$_3$], 12.01 [s, NH$_2$(CH$_2$*Me*)$_2$], 29.86 (m, dppe CH$_2$), 43.32 [s, NH$_2$(*CH$_2$*Me)$_2$], 124.46–132.27 (m, dppe Ph). ^{31}P NMR (d_6-dmso): δ 5.08 [s, *J*(PPt) = 2338 Hz, PEt$_3$], 40.76 [s, *J*(PPt) = 2323 Hz, dppe]. ES mass spectrum (MeCN, *m*/*z*): 2315, [M − OTf]$^+$.

(h) *cyclo*-{Pt$_4$(μ-C≡CC≡C)$_4$(PEt$_3$)$_4$(dppp)$_2$}·[NH$_2$Et$_2$][OTf] 23. Similarly, **3** (96.6 mg, 0.14 mmol) and Pt(OTf)$_2$(PEt$_3$)$_2$ (100 mg, 0.14 mmol) gave cream *cyclo*-{Pt$_4$(μ-C≡CC≡C)$_4$(PEt$_3$)$_4$(dppp)$_2$}·[NH$_2$Et$_2$][OTf] **23** (193 mg, 57%). Anal. Found: C, 47.98; H, 4.81; N, 0.56. $C_{99}H_{124}F_3NO_3P_8Pt_4S$ calc.: C, 47.69; H, 5.01; N, 0.56%; *M*, 2493. IR (Nujol): *ν*(C≡C) 2149m, *ν*(OTf) 1290m, 1224m, 1029m cm^{-1}. ^{1}H NMR (d_6-dmso): δ 1.08 [m, 36H, P(CH$_2$*Me*)$_3$], 1.22 [m, 6H, NH$_2$(CH$_2$*Me*)$_2$], 1.72 [m, 6H, NH$_2$(CH$_2$*Me*)$_2$], 1.96 [m, 24H, P(*CH$_2$*Me)$_3$], 2.99 (m, 12H, dppp CH$_2$), 7.12–7.71 (m, 40H, dppp Ph). ^{13}C NMR (d_6-dmso): δ 8.13 [s, P(CH$_2$*Me*)$_3$], 11.17 [s, NH$_2$(CH$_2$*Me*)$_2$], 16.14 [s, P(*CH$_2$*Me)$_3$], 24.00 (m, dppp CH$_2$), 41.62 [s, NH$_2$(*CH$_2$*Me)$_2$], 92.38 (m, C≡C), 118.53 (m, C≡C), 127.85–133.51 (m, dppp Ph). ^{31}P NMR (d_6-dmso): δ −7.69 [s, *J*(PPt) = 2284 Hz, dppp], 6.15 [s, *J*(PPt) = 2209 Hz, PEt$_3$]. ES mass spectrum (MeCN, *m*/*z*): 2343, [M − OTf]$^+$.

(i) *cyclo*-{Pt$_4$(μ-C≡CC≡C)$_4$(dppe)$_2$(dppp)$_2$}·[NH$_2$Et$_2$][OTf] 24. Similarly, **2** (76 mg, 0.11 mmol) and Pt(OTf)$_2$(dppp) (100 mg, 0.11 mmol) gave cream *cyclo*-{Pt$_4$(μ-C≡CC≡C)$_4$(dppe)$_2$(dppp)$_2$]·[NH$_2$Et$_2$][OTf] **27** (169 mg, 60%). Anal. Found: C, 53.94; H, 4.05; N, 0.69. $C_{127}H_{112}F_3NO_3P_8Pt_4S$ calc.: C, 54.14; H, 4.00; N, 0.50%; *M*, 2814. IR (Nujol): *ν*(C≡C) 2149m, 2086m, *ν*(OTf) 1286m, 1244m, 1029m cm^{-1}. ^{1}H NMR (d_6-dmso): δ 1.17 [t, 6H, *J*(HH) = 9 Hz, NH$_2$(CH$_2$CH$_3$)$_2$], 2.53 (m, CH$_2$), 2.91 [m, 4H, NH$_2$(*CH$_2$*CH$_3$)$_2$], 6.92–7.83 (m, 20H, Ph). ^{13}C NMR (d_6-dmso): δ 11.30 [s, NH$_2$(CH$_2$C*H$_3$*)$_2$], 28.56 (m, CH$_2$ dppp). 29.45 (m, CH$_2$ dppe), 41.64 [s, NH$_2$(*CH$_2$*CH$_3$)$_2$], 100.28 (s, C≡C), 128.38–134.06 (m, Ph). ^{31}P NMR (d_6-dmso): δ 43.36 [s, *J*(PPt) = 2288 Hz, dppe], −3.45 [s, *J*(PPt) = 3408 Hz, dppp]. ES mass spectrum (CH$_2$Cl$_2$–MeOH, *m*/*z*): 2667, [M − OTf]$^+$.

Formation of adducts with Group 11 cations

(a) [{Pt(C≡CC≡C)(dppe)}$_4$Cu][NH$_2$Et$_2$][OTf]$_2$ 25. Compound **2** (77.5 mg, 0.11 mmol) and {Cu(OTf)}$_2$(C$_6$H$_6$) (24 mg, 0.11 mmol) were dissolved in CH$_2$Cl$_2$ (50 ml) and NHEt$_2$ (1 ml). To this solution, Pt(OTf)$_2$(dppe) (100 mg, 0.11 mmol) in CH$_2$Cl$_2$ (10 ml) was added *via* syringe pump over a period of 2 h. The initial pale yellow solution darkened to orange–brown. The solvent was reduced to *ca.* 5 ml and filtered into rapidly stirred cold hexane, to give a light brown precipitate of [{Pt(C≡CC≡C)(dppe)}$_4$Cu][NH$_2$Et$_2$][OTf]$_2$ **25** (202 mg, 65%). Anal. Found: C, 50.21; H, 3.80; N, 0.60. $C_{126}H_{108}CuF_6NO_6P_8Pt_4S_2$ calc.: C, 50.41; H, 3.63; N, 0.46%, *M*, 2778. IR (Nujol): *ν*(C≡C) 2127m, 2088m, *ν*(OTf) 1280m, 1261m, 1224m, 1030m cm^{-1}. ^{1}H NMR (d_6-dmso): δ 3.05 (q, 4H, CH$_2$), 7.11–7.83 (m, 20H, Ph). ^{13}C NMR (d_6-dmso): δ 27.40 (m, CH$_2$ dppe), 127.06–133.32 (m, Ph). ^{31}P NMR (d_6-dmso): δ 43.243 [s, *J*(PPt) = 2246 Hz, dppe], 46.40 [s, *J*(PPt) = 3598 Hz, dppe]. ES mass spectrum (MeCN, *m*/*z*; M ≡ **20**): 2629, [M + Cu]$^+$.

(b) [{Pt(C≡CC≡C)(dppe)}$_4$Ag][NH$_2$Et$_2$][OTf]$_2$ 26. Similarly, addition of Pt(OTf)$_2$(dppe) (100 mg, 0.11 mmol in CH$_2$Cl$_2$ (10 ml) to **2** (77.5 mg, 0.11 mmol) and Ag(OTf) (29 mg, 0.11 mmol) in CH$_2$Cl$_2$ (50 ml) containing NHEt$_2$ (1 ml) gave cream [{Pt(C≡CC≡C)(dppe)}$_4$Ag][NH$_2$Et$_2$][OTf]$_2$ **26** (300 mg, 95%). Anal. Found: C, 49.56; H, 3.09; N, 0.60. $C_{126}H_{108}AgF_6NO_6P_8Pt_4S_2$ calc.: C, 49.68; H, 3.57; N, 0.46%; *M*, 3046. IR (Nujol): *ν*(C≡C) 2147m, 2088m, *ν*(OTf) 1271m, 1248m, 1226m, 1031m cm^{-1}. ^{1}H NMR (d_6-dmso): δ 3.07 (m, 4H, CH$_2$), 6.85–7.49 (m, 20H, Ph). ^{13}C NMR (d_6-dmso): δ 10.96 [s, NH$_2$(CH$_2$*Me*)$_2$], 28.56 (m, CH$_2$), 41.34 [s, NH$_2$(*CH$_2$*Me)$_2$], 128.42–133.32 (m, PPh$_2$). ^{31}P NMR (d_6-dmso): δ 42.21 [s, *J*(PPt) = 2336 Hz, dppe], 44.24 [s, *J*(PPt) = 3652 Hz, dppe]. ES mass spectrum (MeCN, *m*/*z*; M ≡ **20**): 1356, [M + Ag(MeCN)]$^{2+}$; 1335, [M + Ag]$^{2+}$.

(c) [{Pt(C≡CC≡C)(dppe)}$_4${Cu(NCMe)}$_2$][BF$_4$]$_2$ 27. A solution of [Cu(NCMe)$_4$][BF$_4$] (24 mg, 0.12 mmol) and **17** (75 mg, 0.03 mmol) in CH$_2$Cl$_2$ (20 ml) was stirred at room temperature for 1 h, after which solvent was removed. A filtered CH$_2$Cl$_2$ extract was added dropwise to cold rapidly stirred Et$_2$O (100 ml) to give a cream precipitate of [{Pt(C≡CC≡C)(dppe)}$_4${Cu(NCMe)}$_2$][BF$_4$]$_2$ **27** (32 mg, 37%). Anal. Found: C, 51.97; H, 3.71, N, 0.71. $C_{124}H_{102}B_2Cu_2F_8N_2P_8Pt_4$ calc.: C, 50.50; H, 3.48; N, 0.94%; *M*, 2949. IR (Nujol): *ν*(C≡C) 2087m, *ν*(BF) 839s cm^{-1}. ^{1}H NMR (d_6-dmso): δ 2.5 (s, 3H, *Me*CN), 2.99 (m, 4H, CH$_2$), 7.19–7.89 (m, 20H, Ph). ^{13}C NMR (d_6-dmso): δ, CH$_2$), 121.89 (s, Me*C*N), 127.85–134.11 (m, dppe Ph). ^{31}P NMR (d_6-dmso): δ 40.03 [s, *J*(PPt) = 2275 Hz, dppe], 43.35 [s, *J*(PPt) = 3604 Hz, dppe]. ES mass spectrum (MeCN, *m*/*z*; M ≡ **20**): 1388, [M + 2Cu(MeCN)]$^{2+}$.

(d) [{Pt(C≡CC≡C)(dppe)}$_4${Ag(NCMe)}$_4$][BF$_4$]$_4$ 28. Similarly, [Ag(NCMe)$_4$][BF$_4$] (57 mg, 0.16 mmol) and **17** (100 mg, 0.04 mmol) in CH$_2$Cl$_2$ (20 ml) gave cream [{Pt(C≡CC≡C)(dppe)}$_4${Ag(NCMe)}$_4$][BF$_4$]$_4$ **28** (95 mg, 67%). The compound darkens upon standing, eventually turning black, and consistent elemental analyses have not been obtained. IR (Nujol): *ν*(C≡C) 2097m, *ν*(BF) 823s cm^{-1}. ^{1}H NMR (d_6-dmso): δ 2.09 (s, 3H, *Me*CN), 2.54 (m, 4H, CH$_2$), 7.20–8.37 (m, 20H, Ph). ^{13}C NMR (d_6-dmso): δ 28.36 (m, CH$_2$), 127.72–134.84 (m, PPh$_2$). ^{31}P NMR (d_6-dmso): δ 42.40 [s, *J*(PPt) = 2421 Hz, dppe]. ES mass spectrum (MeCN, *m*/*z*): 3156, [M + 4Ag + 4MeCN]$^+$; 3115, [M + 4Ag + 3MeCN]$^+$; 1535, [M + 4Ag + 2MeCN]$^{2+}$.

ES mass spectrometry

Stock solutions of **2** (0.01 M in MeOH) and of each cation (0.005 M in 1 : 1 MeOH : H$_2$O, were prepared using the chlorides (except for Rb$^+$, for which RbNO$_3$) were used. The latter were also used to prepare the mixed cation solution (0.005 M). Aliquots of **2** (1 ml) and the cations (0.5 ml) were mixed, stirred for 5 min and the ES mass spectra were measured. Similarly,

Table 4 Crystal and refinement data

	1	**2**	**3**	**5**	**17** ($P2_1/c$)	**17** ($P\bar{1}$)
Formula	$C_{20}H_{32}P_2Pt{\cdot}0.5CH_2C_2$	$C_{34}H_{26}P_2Pt{\cdot}$ $2CH_2Cl_2$	$C_{35}H_{28}P_2Pt$	$C_{92}H_{70}Co_4O_8P_6Pt$	$C_{120}H_{96}P_8Pt_4{\cdot}$ $\approx 4.5dmso{\cdot}H_2O$	$C_{120}H_{96}P_8Pt_4{\cdot}$ 10dmso
M	571.97	861.49	705.64	1920.22	2974.89	3347.55
Crystal system	Tetragonal	Monoclinic	Monoclinic	Monoclinic	Monoclinic	Triclinic
Space group	$P4_2/nmc$	$C/2c$	$P2_1/n$	$P2_1/c$	$P2_1/c$	$P\bar{1}$
a/Å	12.3036(8)	28.611(16)	9.683(4)	21.486(4)	21.524(1)	13.127(2)
b/Å		8.958(3)	22.496(5)	13.439(2)	30.235(2)	17.201(3)
c/Å	16.455(1)	14.718(14)	12.993(4)	29.592(3)	19.155(1)	17.570(3)
α/°						70.582(3)
β/°		109.59(6)	93.65(3)	99.160(2)	91.937(1)	68.705(3)
γ/°						87.309(3)
V/Å^3	2491	3554	2824	8436	12458	3474
Z	4	4	4	4		1
D_c/g cm^{-3}	1.525	1.610	1.659	1.512	1.564	1.600
F(000)	1124	1552	1384	3848	5780	1668
Crystal size/mm	0.65 × 0.24 × 0.21	0.40 × 0.22 × 0.65	0.32 × 0.66 × 0.11	0.50 × 0.22 × 0.10	0.35 × 0.10 × 0.10	0.30 × 0.20 × 0.10
T^* (min, max)	0.523, 0.894	0.233, 0.927	0.568, 0.730	0.336, 0.831	0.600, 0.831	0.633, 0.914
μ/cm^{-1}	58.7	43.6	51.0	25.92	47.1	43.1
$2\theta_{max}$/°	58	60	50	58	50	58
N_{total}	26428		9558	70532	139421	40676
N (R_{int})	1787 (0.026)	5002	4967 (0.039)	21268 (0.078)	21456 (0.040)	17074 (0.039)
N_o	1288	3371	3422	5261	9947	11568
R	0.017	0.071	0.037	0.092	0.052	0.061
R_w	0.034	0.074	0.041	0.112	0.050	0.069

0.005 M solutions of $[M^I(NCMe)_4]BF_4$ (M^I = Cu, Ag) in MeOH were mixed with an equimolar amount of **2** in the same solvent, and the relative intensities of the $[M^2 + M^I]^+$ peaks were recorded.

Structure determinations

For **2** and **3**, room-temperature single counter diffractometer data sets (*T ca.* 295 K; $2\theta/\theta$ scan mode, $2\theta_{max}$ as specified) were measured to the specified level of redundancy, N_{total} reflections (where other than unique) being merged after gaussian absorption correction, to N unique (R_{int} cited where appropriate), N_o with $I > 3\sigma(I)$ being used in the full matrix least squares refinement on $|F|$, minimising $\Sigma w\Delta^2$ and refining anisotropic thermal parameters for the non-hydrogen atoms, $(x, y, z, U_{iso})_H$ being constrained at estimates. For the remainder, full spheres of data to $2\theta = 58°$ were measured at *ca.* 153 K using a Bruker AXS CCD area-detector instrument, merged to unique sets after "empirical"/multiscan absorption corrections (proprietary software), N_{tot} data giving N unique (R_{int} quoted), N_o with $F > 4\sigma(F)$ being used in the refinements. All data were measured using monochromatic Mo-Kα radiation, $\lambda = 0.7107_3$ Å.

In all cases, conventional residuals R, R_w on $|F|$ (statistical weights) are quoted. Neutral atom complex scattering factors were used; computation used the XTAL 3.4 program system.[57] Crystal and refinement data are given in Table 4 and pertinent structural results are given in Figs. 1–3, 5 and 7 [which show 20% (room temperature) or 50% (low temperature) thermal envelopes for the non-hydrogen atoms, hydrogen atoms having arbitrary radii of 0.1 Å)] and Tables 1–3. Individual variations in procedures, abnormalities, idiosyncrasies, *etc.*, are as follows:

1: Difference map residues about (3/4, 1/4, 1/4) (*etc.*) were modelled as disordered dichloromethane of solvation.

2: Specimens were problematically twinned, one deconvoluted reciprocal lattice component being used with separate scale factors in refinement for *hk* ± 1, ±2 (*k* < 6). An analytical absorption correction was applied.

3: A hemisphere of data was measured; an analytical absorption correction was applied.

5: Weak and limited data would support meaningful anisotropic displacement parameter refinement for Pt, Co, P only.

17·10dmso: Phenyl ring 212 and dmso molecules 4, 5 were each modelled as disordered over two sets of sites, occupancies set at 0.5 after trial refinement. Similarly, in **17**·4.5dmso·H$_2$O (T = 300 K), rings 211, 212, 411 and dmso 3, 4 (S only) were modelled as disordered, dmso 5 with site occupancy 0.5. Geometries of the components of ring 411, 411′ were constrained in refinement.

CCDC reference numbers 169975–169980.

See http://www.rsc.org/suppdata/dt/b1/b107929h/ for crystallographic data in CIF or other electronic format.

Theoretical calculations

Extended Hückel calculations were carried out on the model complexes Pt(C≡CC≡CH)$_2$(dHpe) (**2-H**) of C_{2v} symmetry and *cyclo*-{Pt(μ-C≡CC≡C)(dHpe)}$_4$ (**17-H**) of D_{4h} symmetry within the extended Hückel formalism[58] using the program CACAO.[59] Standard atomic distances were taken. The exponents (ζ) and the valence shell ionisation potentials (H_{ii} in eV) were respectively: 1.3, −13.6 for H 1s; 1.625, −21.4 for C 2s; 1.625, −11.4 for C 2p; 1.6, −18.6 for P 3s; 1.6, −14.0 for P 3p; 2.55, −9.077 for Pt 6s; 2.554, −5.475 for Pt 6p. The H_{ii} value for Pt 5d was set equal to −12.59. A linear combination of two Slater-type orbitals with exponents $\zeta = 6.013$ and $\zeta_2 = 2.696$ with the weighting coefficients $c_1 = 0.6334$ and $c_2 = 0.5513$ was used to represent the Pt 5d atomic orbitals.

Density functional calculations were carried out on the model complexes Pt(C≡CC≡CH)$_2$(dHpp) (**3-H**) of C_{2v} symmetry and *cyclo*-{Pt(μ-C≡CC≡C)(dHpe)}$_4$ (**17-H**) of D_{4h} symmetry using the Amsterdam Density Functional (ADF) program[60] developed by Baerends and coworkers.[61] The Vosko–Wilk–Nusair parametrisation[62] was used for the local density approximation (LDA) with gradient corrections for exchange (Becke88)[63] and correlation (Perdew86).[64] The geometry optimisation procedure was based on the method developed by Vesluis and Ziegler.[65] The scalar relativistic effects[66] were taken into account by use of the quasi-relativistic method.[67] The electronic configurations of the molecular systems were described by a double-ζ Slater-type orbital (STO) basis set for H (1s) and C (2s, 2p) of the dHpe and dHpp ligands, whereas an uncontracted triple-ζ basis set was used for P (3s, 3p) of the dHpe and dHpp ligands and for C (2s, 2p) of the C$_4$H chains, augmented with a 3d polarisation function. An uncontracted triple-ζ Slater-type orbital (STO) basis set was used for Pt 5d and 6s atomic orbitals, augmented with a single-ζ 6p function. A frozen-core approximation was used to treat the core electrons of C, P and Pt.[61] The adiabatic ionisation potential computed for model **20-H** was defined as the energy difference between optimised geometries of the reduced and oxidised species.

Acknowledgements

We thank the Australian Research Council for support of this work and Professor M.A. Bennett (Research School of Chemistry, Australian National University, Canberra) for a sample of *cis*-$PtCl_2(PEt_3)_2$. BCH and PJL acknowledge receipt of Postgraduate Research Awards. KC and J-FH thank the Centre de Ressources Informatique (CRI) of Rennes and the Institut de Développment et de Ressources en Informatique Scientifique (IDRIS-CNRS) of Orsay for computing facilities. These studies were also facilitated by travel grants (ARC IREX, Australia, and the Centre National de la Recherche Scientifique, France).

References

1 (*a*) P. J. Stang and B. Olenyuk, *Acc. Chem. Res.*, 1997, **30**, 502; (*b*) S. Leininger, B. Olenyuk and P. J. Stang, *Chem. Rev.*, 2000, **100**, 853.

2 (*a*) M. Fujita, J. Yazaki and K. Ogura, *J. Am. Chem. Soc.*, 1990, **112**, 5645; (*b*) M. Fujita, in *Comprehensive Supramolecular Chemistry*, ed. J. L. Atwood, J. E. D. Davies, D. D. MacNicol and F. Vögtle, Pergamon, Oxford, 1996, vol. 9, ch. 7, p. 253.

3 (*a*) P. J. Stang, D. H. Cao, S. Saito and A. M. Arif, *J. Am. Chem. Soc.*, 1995, **117**, 6273; (*b*) P. J. Stang and J. A. Whiteford, *Organometallics*, 1994, **13**, 2524; (*c*) J. A. Whiteford, C. V. Lu and P. J. Stang, *J. Am. Chem. Soc.*, 1997, **119**, 2524.

4 (*a*) Y. Fujikura, K. Sonogashira and N. Hagihara, *Chem. Lett.*, 1975, 1067; (*b*) K. Sonogashira, N. Takahashi and N. Hagihara, *Macromolecules*, 1977, **10**, 879; (*c*) K. Sonogashira, T. Yatake, T. Tohda, S. Takahashi and N. Hagihara, *J. Chem. Soc., Chem. Commun.*, 1977, 291; (*d*) K. Sonogashira, S. Kataoka, S. Takahashi and N. Hagihara, *J. Organomet. Chem.*, 1978, **160**, 319; (*e*) K. Sonogashira, K. Ohga, S. Takahashi and N. Hagihara, *J. Organomet. Chem.*, 1980, **188**, 237; (*f*) S. Takahashi, Y. Ohyama, E. Murata, K. Sonogashira and N. Hagihara, *Polym. Sci., Polym. Chem. Ed.*, 1980, **18**, 339; (*g*) S. Takahashi, E. Murata, K. Sonogashira and N. Hagihara, *Polym. Sci., Polym. Chem. Ed.*, 1980, **18**, 661; (*h*) S. Takahashi, H. Morimoto, E. Murata, S. Kataoka, K. Sonogashira and N. Hagihara, *Polym. Sci., Polym. Chem. Ed.*, 1982, **20**, 565.

5 (*a*) B. F. G. Johnson, A. K. Kakkar, M. S. Khan, J. Lewis, A. E. Day, R. H. Friend and F. J. Wittmann, *J. Mater. Chem.*, 1991, **1**, 485; (*b*) J. Lewis, M. S. Khan, A. K. Kakkar, B. F. G. Johnson, T. B. Marder, H. B. Fyfe, F. W. Wittmann, R. H. Friend and A. E. Day, *J. Organomet. Chem.*, 1992, **425**, 165.

6 (*a*) H. Lang, K. Köhler and S. Blau, *Coord. Chem. Rev.*, 1995, **143**, 113; (*b*) H. Lang, D. S. A. George and G. Rheinwald, *Coord. Chem. Rev.*, 2000, **206–207**, 101.

7 (*a*) T. B. Peters, J. C. Bohling, A. M. Arif and J. A. Gladysz, *Organometallics*, 1999, **18**, 3261; (*b*) W. Mohr, J. Stahl, F. Hampel and J. A. Gladysz, *Inorg. Chem.*, 2001, **40**, 3263; (*c*) J. C. Bohling, T. B. Peters, A. M. Arif, F. Hampel and J. A. Gladysz, in *Coordination Chemistry at the Turn of the Century*, ed. G. Ondrejovic and A. Sirota, Slovak Technical University Press, Bratislava, Slovakia, 1999, p. 47.

8 Mo, W: (*a*) B. E. Woodworth, P. S. White and J. S. Templeton, *J. Am. Chem. Soc.*, 1997, **119**, 828; (*b*) M. I. Bruce, M. Ke and P. J. Low, *Chem. Commun.*, 1996, 2405; (*c*) M. I. Bruce, B. C. Hall, P. J. Low, M. E. Smith, B. W. Skelton and A. H. White, *Inorg. Chim. Acta.*, 2000, **300–302**, 633.

9 Mn: S. Kheradmandan, K. Heinze, J. W. Schmalle and H. Berke, *Angew. Chem.*, 1999, **111**, 2412; S. Kheradmandan, K. Heinze, J. W. Schmalle and H. Berke, *Angew. Chem., Int. Ed.*, 1999, **38**, 2270.

10 Re: (*a*) J. W. Seyler, W. Weng, Y. Zhou and J. A. Gladysz, *Organometallics*, 1993, **12**, 3802; (*b*) W. Weng, T. Bartik, M. Brady, B. Bartik, J. A. Ramsden, A. M. Arif and J. A. Gladysz, *J. Am. Chem. Soc.*, 1995, **117**, 11922; (*c*) V. W.-W. Yam, V. C.-Y. Lau and K.-K. Cheung, *Organometallics*, 1996, **15**, 1740.

11 Fe: (*a*) N. Le Narvor, L. Toupet and C. Lapinte, *J. Am. Chem. Soc.*, 1995, **117**, 7129; (*b*) F. Coat and C. Lapinte, *Organometallics*, 1996, **15**, 477; (*c*) F. Coat, M.-A. Guillevic, L. Toupet, F. Paul and C. Lapinte, *Organometallics*, 1997, **16**, 5988; (*d*) M. Guillemot, L. Toupet and C. Lapinte, *Organometallics*, 1998, **17**, 1928.

12 Ru: (*a*) M. I. Bruce, L. I. Denisovich, P. J. Low, S. M. Peregudova and N. A. Ustynyuk, *Mendeleev Commun.*, 1996, 200; (*b*) M. I. Bruce, P. J. Low, K. Costuas, J.-F. Halet, S. P. Best and G. A. Heath, *J. Am. Chem. Soc.*, 2000, **122**, 1949.

13 Ru_2: (*a*) T. Ren, G. Zou and J. C. Alvarez, *Chem. Commun.*, 2000, 1197; (*b*) K.-T. Wong, J.-M. Lehn, S.-M. Peng and G.-H. Lee, *Chem. Commun.*, 2000, 2259.

14 Rh, Ir: (*a*) T. Rappert, O. Nürnberg and H. Werner, *Organometallics*, 1993, **12**, 1359; (*b*) H. Werner, R. W. Lass, O. Gevert and J. Wolf, *Organometallics*, 1997, **16**, 4077.

15 Heterometallic: (*a*) A. Wong, P. C. W. Kang, C. D. Tagge and D. R. Leon, *Organometallics*, 1990, **9**, 1992; (*b*) F. Paul, W. E. Meyer, L. Toupet, H. Jiao, J. A. Gladysz and C. Lapinte, *J. Am. Chem. Soc.*, 2000, **122**, 9405.

16 S. M. AlQaisi, K. J. Galat, M. Chai, D. G. Ray III, P. L. Rinaldi, C. A. Tessier and W. J. Youngs, *J. Am. Chem. Soc.*, 1998, **120**, 12149.

17 A. D. Burrows, D. M. P. Mingos, S. E. Lawrence, A. J. P. White and D. J. Williams, *J. Chem. Soc., Dalton Trans.*, 1997, 1295.

18 D. H. Farrer and G. J. Ferguson, *J. Crystallogr. Spectrosc. Res.*, 1982, **12**, 465.

19 G. B. Robertson and W. A. Wickramasinghe, *Acta. Crystallogr., Sect. C*, 1987, **43**, 1694.

20 M. Bonamico, G. Dessy, V. Fares, M. V. Russo and L. Scaramuzza, *Cryst. Struct. Commun.*, 1977, **6**, 39.

21 (*a*) R. Dembinski, T. Lis, S. Szafert, C. L. Mayne, T. Bartik and J. A. Gladysz, *J. Organomet. Chem.*, 1999, **578**, 229; (*b*) T. B. Peters, J. C. Bohling, A. M. Arif and J. A. Gladysz, *Organometallics*, 1999, **18**, 3261.

22 T. A. Albright, J. K. Burdett and M.-H. Whangbo, *Orbital Interactions in Chemistry*, Wiley, New York, 1985.

23 F. L. Hirshfeld, *Theor. Chem.*, 1977, **44**, 129. In contrast to the Mulliken population analysis, the Hirshfeld method yields atomic charges which are essentially stable against basis set variations and correctly reflect the electronegativity differences between the atoms. See, for example: F. M. Bickelhaupt, N. J. S. van Eikama Hommes, C. F. Guera and E. J. Baerends, *Organometallics*, 1996, **15**, 2923.

24 D. Seyferth, M. O. Nestle and A. T. Wehman, *J. Am. Chem. Soc.*, 1975, **97**, 7417.

25 (*a*) M. I. Bruce, B. D. Kelly, B. W. Skelton and A. H. White, *J. Chem. Soc., Dalton Trans.*, 1999, 847; (*b*) M. I. Bruce, B. C. Hall, B. D. Kelly, P. J. Low, B. W. Skelton and A. H. White, *J. Chem. Soc., Dalton Trans.*, 1999, 3719.

26 (*a*) A. K. Smith, in *Comprehensive Organometallic Chemistry II*, ed. E. W. Abel, F. G. A. Stone and G. Wilkinson, Pergamon, Oxford, 1995, vol. 7, ch. 13, p. 772; (*b*) M. I. Bruce, B. W. Skelton, A. H. White and N. N. Zaitseva, *J. Chem. Soc., Dalton Trans.*, 1996, 3151.

27 M. I. Bruce, P. J. Low, N. N. Zaitseva, S. Kahlal, J.-F. Halet, B. W. Skelton and A. H. White, *J. Chem. Soc., Dalton Trans.*, 2000, 2939.

28 Ref. 6*b*, sect. 2.2, p. 143.

29 J. C. Ma and D. A. Dougherty, *Chem. Rev.*, 1997, **97**, 1303.

30 (*a*) M. Vicenti, *Int. J. Mass Spectrom.*, 1995, **30**, 925; (*b*) J. C. Traeger, *Int. J. Mass Spectrom.*, 2000, **200**, 387.

31 P. A. Brady and J. K. M. Sanders, *New J. Chem.*, 1998, **22**, 411.

32 R. Colton, S. Mitchell and J. C. Traeger, *Inorg. Chim. Acta*, 1995, **231**, 87.

33 K. Wang, X. Han, R. W. Gross and G. W. Gokel, *J. Am. Chem. Soc.*, 1995, **117**, 7680.

34 (*a*) D. S. Young, H. Y. Hung and L. K. Liu, *Int. J. Mass Spectrom.*, 1997, **32**, 432; (*b*) D. S. Young, H. Y. Hung and L. K. Liu, *Rapid Commun. Mass Spectrom.*, 1997, **11**, 769.

35 S. F. Ralph, P. Iannitti, R. Kanitz and M. M. Sheil, *Eur. Mass Spectrom.*, 1996, **2**, 173.

36 (*a*) W. Henderson, B. K. Nicholson and L. J. McCaffrey, *Polyhedron*, 1998, **17**, 4291 and references therein; (*b*) W. Henderson, J. S. McIndoe, B. K. Nicholson and P. J. Dyson, *J. Chem. Soc., Dalton Trans.*, 1998, 519.

37 A. J. Canty and R. Colton, *Inorg. Chim. Acta*, 1994, **220**, 99.

38 (*a*) F. Inokuchi, Y. Miyahara, T. Inazu and S. Shinkai, *Angew. Chem.*, 1995, **107**, 1459; (*b*) F. Inokuchi, Y. Miyahara, T. Inazu and S. Shinkai, *Angew. Chem., Int. Ed. Engl.*, 1995, **34**, 1364.

39 (*a*) E. Bayer, P. Gfrorer and C. Rentel, *Angew. Chem.*, 1999, **111**, 1046; (*b*) E. Bayer, P. Gfrorer and C. Rentel, *Angew. Chem., Int. Ed.*, 1999, **38**, 992.

40 A. J. Canty and R. Colton, *Inorg. Chim. Acta*, 1994, **215**, 179.

41 As in: G. A. Carriedo, D. Miguel, V. Riera and X. Solans, *J. Chem. Soc., Dalton Trans.*, 1987, 2867. See also: (*a*) P. Espinet, J. Forniés, F. Martinez, M. Sotes, E. Lalinde, M. T. Moreno, A. Ruiz and A. J. Welch, *J. Organomet. Chem.*, 1991, **403**, 253; (*b*) O. M. Abu Salah, M. I. Bruce, M. R. Churchill and S. A. Bezman, *J. Chem. Soc., Chem. Commun.*, 1972, 858; (*c*) O. M. Abu Salah, M. I. Bruce, M. R. Churchill and B. G. DeBoer, *J. Chem. Soc., Chem. Commun.*, 1974, 688; (*d*) P. Espinet, J. Fornies, F. Martinez, M. Tomas, E. Lalinde, M. T. Moreno, A. Ruiz and A. J. Welch, *J. Chem. Soc., Dalton Trans.*, 1990, 791.

42 M. I. Bruce, M. Ke, P. J. Low, B. W. Skelton and A. H. White, *Organometallics*, 1998, **17**, 3539.

43 (*a*) G. J. V. Berkel, S. A. McLuckey and G. L. Glish, *Anal. Chem.*, 1992, **64**, 1586; (*b*) G. J. V. Berkel and F. Zhou, *Anal. Chem.*, 1995, **67**, 2916.

44 T. Y. Liu, L. L. Shiu, T. Y. Luh and G. R. Her, *Rapid Commun. Mass Spectrom.*, 1995, **9**, 93.

45 S. J. Cantrill, A. R. Pease and F. J. Stoddart, *J. Chem. Soc., Dalton Trans.*, 2000, 3715 and references 25 and 26 therein.

46 (*a*) D. M. P. Mingos and T. E. Müller, *J. Organomet. Chem.*, 1995, **500**, 251; (*b*) T. E. Müller, S. W.-K. Choi, D. M. P. Mingos, D. Murphy, D. J. Williams and V. W.-W. Yam, *J. Organomet. Chem.*, 1994, **484**, 209; (*c*) T. E. Müller, D. M. P. Mingos and D. J. Williams, *J. Chem. Soc., Chem. Commun.*, 1994, 1787.

47 L. Brunel, F. Carré, S. G. Dutremez, C. Guérin, F. Dahan, O. Eisenstein and G. Sim, *Organometallics*, 2001, **20**, 47.

48 L. Brandsma, *Preparative Acetylenic Chemistry*, Elsevier, Amsterdam, 1971.

49 T. G. Appleton, M. A. Bennett and I. B. Tomkins, *J. Chem. Soc., Dalton Trans.*, 1976, 439.

50 K. Yasufuku, H. Noda and H. Yamazaki, *Inorg. Synth.*, 1989, **26**, 369.

51 D. A. Slack and M. C. Baird, *Inorg. Chim. Acta.*, 1977, **24**, 277.

52 D. Drew and J. R. Doyle, *Inorg. Synth.*, 1990, **28**, 346.

53 L. S. Chia and W. R. Cullen, *Inorg. Chem.*, 1975, **14**, 482.

54 M. I. Bruce, B. K. Nicholson and M. L. Williams, *Inorg. Synth.*, 1989, **26**, 271.

55 G. J. Kubas, *Inorg. Synth.*, 1990, **28**, 68.

56 M. I. Bruce, B. K. Nicholson and O. bin Shawkataly, *Inorg. Synth.*, 1989, **26**, 325.

57 *The XTAL 3.4 Users' Manual*, ed. S. R. Hall, G. S. D. King and J. M. Stewart, University of Western Australia, Lamb, Perth, 1994.

58 R. Hoffmann, *J. Chem. Phys.*, 1963, **39**, 1397.

59 C. Mealli and D. Proserpio, *J. Chem. Educ.*, 1990, **67**, 399.

60 Amsterdam Density Functional (ADF) Program, release 2000. 02, Vrije Universiteit, Amsterdam, The Netherlands.

61 (*a*) E. J. Baerends, D. E. Ellis and P. Ros, *Chem. Phys.*, 1973, **2**, 41; (*b*) E. J. Baerends and P. Ros, *Int. J. Quantum Chem.*, 1978, **S12**, 169; (*c*) P. M. Boerrigter, G. te Velde and E. J. Baerends, *Int. J. Quantum Chem.*, 1988, **33**, 87; (*d*) G. te Velde and E. J. Barends, *J. Comput. Phys.*, 1992, **99**, 84.

62 S. H. Vosko, L. Wilk and M. Nusair, *Can. J. Phys.*, 1980, **58**, 1200.

63 A. D. Becke, *Phys. Rev. A*, 1988, **38**, 3098.

64 J. P. Perdew, *Phys. Rev. B*, 1986, **33**, 8822; J. P. Perdew, *Phys. Rev. B*, 1986, **34**, 7406 (erratum).

65 L. Verluis and T. Ziegler, *J. Chem. Phys.*, 1988, **88**, 322.

66 (*a*) J. G. Snijders and E. J. Baerends, *J. Mol. Phys.*, 1978, **36**, 1789; (*b*) J. G. Snijders, E. J. Baerends and P. Ros, *J. Mol. Phys.*, 1979, **38**, 1909.

67 T. Ziegler, E. J. Baerends, J. G. Snijders and W. Ravenek, *Phys. Chem.*, 1989, **93**, 3050.